

1 **A proteolytic complex targets multiple cell wall hydrolases in**

2 ***Pseudomonas aeruginosa***

3
4
5 **Disha Srivastava^{a*}, Jin Seo^{a*}, Binayak Rimal^b, Sung Joon Kim^c, Andrew J. Darwin^a**

6
7
8 ^a Department of Microbiology, New York University School of Medicine, New York, New
9 York, United States; ^b Institute of Biomedical Studies, Baylor University, Waco, Texas,
10 United States; ^c Department of Chemistry and Biochemistry, Baylor University, Waco,
11 Texas, United States

12
13
14 Running head: Proteolysis of *P. aeruginosa* cell wall hydrolases

15
16
17
18 Address correspondence to: Andrew J. Darwin, andrew.darwin@med.nyu.edu

19
20 * Present addresses: Disha Srivastava, FCBCURE, 5 Sylvan Way, Parsippany, NJ;
21 Jin Seo, Johnson & Johnson Inc., 199 Grandview Road, Skillman, NJ.

22
23 Abstract: 249

24 Text: 6,421 (excluding Abstract, Importance, References, Tables and Figure legends)

25 **ABSTRACT**

26 Carboxy-terminal processing proteases (CTPs) occur in all three domains of life. In
27 bacteria some of them have been associated with virulence. However, the precise roles
28 of bacterial CTPs are poorly understood and few direct proteolytic substrates have been
29 identified. One bacterial CTP is the CtpA protease of *Pseudomonas aeruginosa*, which
30 is required for type III secretion system function, and for virulence in a mouse model of
31 acute pneumonia. Here, we have investigated the function of CtpA in *P. aeruginosa* and
32 identified some of the proteins it cleaves. We discovered that CtpA forms a complex
33 with a previously uncharacterized protein, which we have named LbcA (lipoprotein
34 binding partner of CtpA). LbcA is required for CtpA activity *in vivo* and promotes its
35 activity *in vitro*. We have also identified four proteolytic substrates of CtpA, all of which
36 are uncharacterized proteins predicted to cleave the peptide cross-links within
37 peptidoglycan. Consistent with this, a *ctpA* null mutant was found to have fewer
38 peptidoglycan cross-links than the wild type and grew slowly in salt-free medium.
39 Intriguingly, the accumulation of just one of the CtpA substrates was required for some
40 Δ *ctpA* mutant phenotypes, including the defective T3SS. We propose that LbcA•CtpA is
41 a proteolytic complex in the *P. aeruginosa* cell envelope, which controls the activity of
42 several peptidoglycan cross-link hydrolases by degrading them. Furthermore, based on
43 these and other findings we suggest that many bacterial CTPs might be similarly
44 controlled by partner proteins as part of a widespread mechanism to control
45 peptidoglycan hydrolase activity.

46

47

48 **IMPORTANCE**

49 Bacterial carboxy-terminal processing proteases (CTPs) are widely conserved and have
50 been associated with the virulence of several species. However, their roles are poorly
51 understood and few direct substrates have been identified in any species.
52 *Pseudomonas aeruginosa* is an important human pathogen in which one CTP, known
53 as CtpA, is required for type III secretion system function, and for virulence. This work
54 provides an important advance by showing that CtpA works with a previously
55 uncharacterized binding partner to degrade four substrates. These substrates are all
56 predicted to hydrolyze peptidoglycan cross-links, suggesting that the CtpA complex is
57 an important control mechanism for peptidoglycan hydrolysis. This is likely to emerge as
58 a widespread mechanism used by diverse bacteria to control some of their
59 peptidoglycan hydrolases. This is significant, given the links between CTPs and
60 virulence in several pathogens, and the importance of peptidoglycan remodeling to
61 almost all bacterial cells.

62

63

64 **INTRODUCTION**

65 *Pseudomonas aeruginosa* is a Gram-negative bacterium that accounts for over
66 10% of healthcare associated infections with an identifiable cause (1). In acute
67 infections, *P. aeruginosa* utilizes a type III secretion system (T3SS) to export proteins
68 into host cells, where they interfere with signaling, immune function, and cause
69 cytotoxicity (2). In chronic infections, *P. aeruginosa* forms biofilms resilient to clearance
70 by antibiotics and the immune response (3, 4). The emergence of antibiotic resistant

71 strains is increasing, making this pathogen a top priority for the discovery of new
72 therapeutic targets (5).

73 Proteases are important virulence factors for many pathogens, including *P.*
74 *aeruginosa* (6). One intriguing family is the carboxy-terminal processing proteases
75 (CTPs), found in all three domains of life. CTPs belong to the S41 family of serine
76 proteases with a serine/lysine catalytic dyad (7). They are believed to target substrates
77 close to their C-terminus (8, 9). A well described CTP occurs in plant chloroplasts and
78 cyanobacteria, where it cleaves a component of the photosystem II reaction center to
79 activate it (10, 11). Gram-negative bacterial CTPs are found exclusively in the
80 periplasmic compartment and have been implicated in cleaving proteins associated with
81 cell envelope function (8, 12). Some CTPs have been associated with virulence, but
82 mostly by poorly defined mechanisms (13-19). Indeed, despite their widespread
83 conservation, our knowledge of how CTPs function, and what they cleave, is limited.

84 *Escherichia coli* has one CTP, known as Prc or Tsp (8, 9). *prc* null mutants have
85 altered cell morphology, increased drug and low osmotic sensitivity, and altered
86 virulence (20, 21). Prc was proposed to process penicillin binding protein 3 (FtsI), an
87 essential peptidoglycan transpeptidase required for cell division (8). More recently
88 another Prc substrate was discovered, the peptidoglycan hydrolase MepS, which
89 cleaves peptide cross-links between the glycan chains of peptidoglycan (22, 23). These
90 substrates suggest that Prc plays a role in controlling different aspects of peptidoglycan
91 metabolism. However, Prc has also been shown to cleave incorrectly folded
92 polypeptides in the periplasm, suggesting that it has a broader role in protein quality
93 control (9, 24, 25). *P. aeruginosa* has a homolog of *E. coli* Prc, with the two proteins

94 sharing over 40% amino acid identity and belonging to the CTP-1 subfamily (7). *P.*
95 *aeruginosa* Prc has been proposed to contribute to degradation of the antisigma factor
96 MucA, which induces the AlgT/U regulon and subsequent production of the
97 exopolysaccharide, alginate (26-28).

98 Unlike *E. coli*, *P. aeruginosa* has a second CTP, CtpA, which is smaller than Prc
99 and in a different subfamily (the CTP-3 subfamily; 18, 29). CtpA is required for T3SS
100 function, and a *ctpA* null mutant is less cytotoxic to cultured cells and attenuated in a
101 mouse model of acute pneumonia (18). We also reported that a Δ *ctpA* mutant is
102 sensitive to mislocalized pore forming secretin proteins, has increased resistance to two
103 cationic surfactants, has an altered cell envelope when viewed by electron microscopy,
104 and that CtpA overproduction induces an extracytoplasmic function sigma factor regulon
105 (18). Furthermore, others found that a *ctpA* transposon insertion mutant has reduced
106 swarming motility (30). All of this suggests that CtpA has a significant impact on the cell
107 envelope. Here, we report that CtpA forms a complex with a protein we have named
108 LbcA (lipoprotein binding partner of CtpA). LbcA is required for CtpA activity *in vivo* and
109 promotes its activity *in vitro*. We have also identified four substrates of CtpA, all of which
110 are uncharacterized proteins predicted to cleave the peptide cross-links within
111 peptidoglycan. The accumulation of one of these substrates appears to be needed for
112 some of the most significant phenotypes of a Δ *ctpA* mutant, including the defective
113 T3SS. We argue that many bacterial CTPs might be controlled by partner proteins as
114 part of a widespread mechanism to control peptidoglycan hydrolase activity.

115

116

117 RESULTS

118 **Identification of a CtpA binding partner.** We modified the chromosomal *ctpA*
119 gene to encode CtpA-FLAG-His₆, in strains encoding wild type CtpA or CtpA-S302A
120 (catalytic serine mutated to alanine). The rationale was that CtpA-S302A might trap
121 substrates after tandem affinity purification. These experiments were done with or
122 without *in vivo* formaldehyde cross-linking prior to protein purification, but the results
123 were similar and only an experiment without cross-linking is shown (Fig. 1A).

124 Both versions of CtpA co-purified with abundant amounts of a protein running
125 between 50 and 75 kDa markers in SDS-PAGE (Fig. 1A). Mass spectrometry identified
126 it as PA4667 (PAO1 strain designation). A polyclonal antiserum raised against PA4667
127 confirmed its co-purification with epitope tagged CtpA or CtpA-S302A (Fig 1B). PA4667
128 is a predicted 63 kDa outer membrane lipoprotein with eleven tetratricopeptide (TPR)
129 repeats. The TPR motif is a degenerate 34 amino acid sequence that mediates protein-
130 protein interactions (31). PA4667 does not appear to be a CtpA substrate because its
131 level is similar in *ctpA*⁺ and Δ *ctpA* strains (see below). Therefore, we will refer to
132 PA4667 as LbcA, (lipoprotein binding partner of CtpA).

133 **Δ *lbcA* and Δ *ctpA* mutants have common phenotypes.** We hypothesized that
134 LbcA might be required for CtpA function, but we could not construct Δ *lbcA* in frame
135 deletion mutants. We could make mutants where *lbcA* was replaced by *aacC1*,
136 encoding gentamycin resistance, but only if *aacC1* was in the same orientation as *lbcA*.
137 *lbcA* is in an operon with the downstream essential genes, *lolB* and *ipk* (32). We
138 speculate that the *aacC1* promoter helps to express *lolB-ipk*, and the inability to make a
139 Δ *lbcA* in frame deletion might be due to reduced *lolB-ipk* expression.

140 A $\Delta ctpA$ mutant has a defective T3SS (18). Therefore, we compared the ability of
141 *ctpA* and *lbcA* null mutants to export T3SS effector proteins ExoS and ExoT and found
142 that both were defective (Fig. 2A). The $\Delta lbcA::aacC1$ mutant was complemented by an
143 *lbcA*⁺ plasmid, and the $\Delta ctpA$ mutant was complemented by wild type CtpA but not by
144 CtpA-S302A (Fig. 2A).

145 Recently, we discovered that a $\Delta ctpA$ mutant has a phenotype in a commonly
146 used surface attachment assay (33). After an 8 hour incubation, the $\Delta ctpA$ mutant
147 attached robustly whereas the wild type did not (Fig. 2B). We tested if the *lbcA* null
148 mutant shares this phenotype, and it did (Fig. 2B). After longer incubation the wild type
149 caught up so that attachment of wild type and mutant strains was indistinguishable (data
150 not shown). This accelerated attachment phenotype was not caused by faster growth of
151 the mutants in these assays (data not shown).

152 **Evidence that LbcA recruits CtpA to the outer membrane.** LbcA is a
153 predicted outer membrane lipoprotein, so it should tether CtpA to the membrane.
154 However, we and others concluded that CtpA is a soluble periplasmic protein because it
155 was released by osmotic shock (18, 29). Even so, some CtpA was not released in our
156 experiment (18). Indeed, we have found that a significant amount of CtpA is always
157 retained, and this is more pronounced when cultures are harvested at a lower optical
158 density (OD) than before (OD 600nm of 1 instead of 1.5). Therefore, we osmotically
159 shocked *lbcA*⁺ and $\Delta lbcA$ strains grown to OD 600 nm of 1. In the *lbcA*⁺ strain, most
160 CtpA was retained, whereas a soluble periplasmic control protein was released (Fig.
161 3A). However, in an $\Delta lbcA$ mutant, CtpA was released. This supports the hypothesis
162 that LbcA influences CtpA localization.

163 We also separated cells into soluble and insoluble fractions by lysis and
164 ultracentrifugation. Interestingly, LbcA was found in the soluble and insoluble fractions
165 (Fig. 3B). We do not know if this is physiologically significant, or an artifact resulting
166 from LbcA being solubilized during sample processing. Regardless, in an *lbcA*⁺ strain,
167 CtpA fractionated identically to LbcA, whereas in an Δ *lbcA* mutant CtpA was only in the
168 soluble fraction (Fig. 3B). This is also consistent with an LbcA•CtpA interaction tethering
169 some CtpA to the outer membrane.

170 **Isolation of a putative CtpA substrate.** To find substrates of the LbcA•CtpA
171 complex, we modified our tandem affinity tag approach by putting the His₆ tag on CtpA
172 or CtpA-S302A, and the FLAG tag on LbcA. Strains were grown in T3SS inducing
173 conditions and treated with formaldehyde to cross-link associated proteins. Proteins
174 were purified using nickel agarose followed by anti-FLAG affinity gel and analyzed by
175 SDS-PAGE (Fig. 4A). We also analyzed two independent purifications from each strain
176 by mass spectrometry. 101 proteins were present in both LbcA•CtpA-S302A samples,
177 but neither LbcA•CtpA sample (Fig. 4B and Supplemental Table 1). We focused on the
178 most abundant according to peptide spectrum matches (PSMs), the uncharacterized
179 PA0667 (Fig. 4B). PA0667 has a Sec-dependent signal sequence, a LysM
180 peptidoglycan-binding domain, and a LytM/M23 peptidase domain. It is 35% identical to
181 *E. coli* MepM, a DD-endopeptidase that cleaves D-Ala-meso-DAP peptide peptidoglycan
182 cross-links (23). Therefore, we will refer to PA0667 as MepM.

183 **Evidence that MepM is a substrate of the LbcA•CtpA complex *in vivo*.** To
184 test if MepM might be an LbcA•CtpA substrate, we constructed a plasmid encoding
185 arabinose inducible MepM-FLAG. After growth in the presence of arabinose the MepM-

186 FLAG protein was undetectable in the wild type strain, whereas it was abundant in
187 $\Delta ctpA$ and $\Delta lbcA$ mutants (Fig. 4C). To analyze endogenous MepM, we raised a
188 polyclonal antiserum against it. This antiserum did not detect MepM in the wild type
189 strain, but once again it revealed MepM accumulated in a $\Delta ctpA$ mutant (Fig. 4D). This
190 accumulation was reversed by a plasmid encoding wild type CtpA, but not by CtpA-
191 S302A (Fig 4D). These data suggest that MepM is cleaved by CtpA *in vivo*.

192 **Deletion of *mepM* suppresses $\Delta ctpA$ mutant phenotypes.** $\Delta ctpA$ phenotypes
193 might be caused by MepM accumulation. If so, a $\Delta mepM$ mutation should suppress
194 them. To test this, we introduced a *mepM* in frame deletion mutation into wild type and
195 $\Delta ctpA$ strains and surveyed their phenotypes (Fig. 5).

196 First, we monitored T3SS function. The $\Delta mepM$ mutation alone did not affect
197 ExoS/T export (Fig. 5A), whereas a $\Delta ctpA$ mutant exported lower amounts, as reported
198 before (18). However, the $\Delta ctpA$ phenotype was suppressed by a $\Delta mepM$ mutation, with
199 the ExoS/T secretion profiles of wild type and $\Delta ctpA \Delta mepM$ strains being
200 indistinguishable (Fig. 5A). Furthermore, *mepM* expression from a plasmid reduced
201 T3SS function in the $\Delta ctpA \Delta mepM$ mutant (Fig 5A). These data suggest that MepM
202 accumulation was responsible for the defective T3SS of the $\Delta ctpA$ mutant.

203 We also investigated cytotoxicity towards CHO-K1 cells by measuring lactate
204 dehydrogenase (LDH) release. This is an established model for studying the toxic effect
205 of the *P. aeruginosa* T3SS on eukaryotic cells (18, 34). The cytotoxicity phenotypes of
206 the $\Delta ctpA$, $\Delta mepM$ and $\Delta ctpA \Delta mepM$ strains were consistent with their T3SS
207 phenotypes (Figs. 5A and B). $\Delta mepM$ did not affect cytotoxicity, $\Delta ctpA$ reduced it, and
208 this reduction was suppressed in the $\Delta ctpA \Delta mepM$ double mutant (Fig. 5B).

209 Finally, the $\Delta mepM$ mutation also suppressed the accelerated surface
210 attachment phenotype of a $\Delta ctpA$ mutant, and this suppression was reversed by a
211 $mepM^+$ plasmid (Fig. 5C). Together, all these findings suggest that many phenotypes of
212 a $\Delta ctpA$ mutant require MepM. As expected, a $\Delta mepM$ mutation also suppressed these
213 phenotypes of a $\Delta lbcA$ mutant (data not shown). Therefore, we hypothesized that the
214 phenotypes of LbcA•CtpA-defective strains are the result of increased hydrolysis of
215 peptidoglycan cross-links, which we tested next.

216 **Peptidoglycan cross-linking is reduced in a $\Delta ctpA$ mutant.** The
217 peptidoglycan compositions of wild type and $\Delta ctpA$ strains were characterized by mass
218 spectrometry. The repeat unit consists of the disaccharide GlcNAc-MurNAc with a
219 pentapeptide stem L-Ala-D-iso-Gln-*m*-Dap-D-Ala-D-Ala attached to the lactic moiety of
220 MurNAc (Fig. 6A). The disaccharides are joined by β_{1-4} glycosidic linkages to form the
221 glycan chain. The glycan chains are cross-linked via a peptide bond between the
222 sidechain of *m*-DAP in an acceptor stem of one repeat unit, to the carbonyl carbon of a
223 penultimate D-Ala in a donor stem of a neighboring glycan chain. Cell walls were
224 digested with mutanolysin, which cleaves the β_{1-4} glycosidic linkage between MurNAc
225 and GlcNAc, resulting in muropeptide fragments with intact cross-links. Muropeptide
226 ions were identified by matching the observed *m/z* values to the corresponding entries
227 in a muropeptide library generated *in silico* using an in-house program. Forty-seven
228 unique muropeptide ion species from the wild type, and thirty-three from the $\Delta ctpA$
229 mutant were selected for the analysis. Muropeptide fragments were quantified by
230 integrating the extracted ion chromatogram (XIC) of the selected muropeptide ion (35-
231 37). The normalized summed integrals of muropeptides from the XIC ion current were

232 categorized based on the cross-link number per muuropeptide fragment (Fig. 6B).
233 Muuropeptide fragments larger than trimers were not observed, and the most abundant
234 muuropeptides were dimers. Representative spectra of monomer, dimer, and trimer from
235 the wild type are shown in Figure 6, and the chemical structure and calculated masses
236 are in Supplementary Figure S1.

237 The cell walls of the $\Delta ctpA$ mutant had a reduced concentration of peptidoglycan
238 dimers ($75.85\% \pm 3.90\%$) compared to wild type ($87.30\% \pm 1.34\%$), and a concomitant
239 increase in monomers (Fig. 6B). This is consistent with decreased peptidoglycan cross-
240 linking efficiency (ρ_{CL}) in the $\Delta ctpA$ mutant. The calculated ρ_{CL} for wild type and $\Delta ctpA$
241 mutant were 50.86% and 49.46%, respectively (Fig. 6C). The reduced cross-linking
242 efficiency in the $\Delta ctpA$ mutant is small. However, the accompanying increase in trimers
243 and monomers, indicates altered peptidoglycan biosynthesis. A small effect was
244 expected because a *ctpA* mutant grows well, had few phenotypes in a Biolog
245 Phenotype MicroArray (18), and is only slightly sensitive to low osmotic conditions (see
246 below). Regardless, these data are consistent with the accumulation of peptidoglycan
247 cross-link hydrolase activity in LbcA•CtpA-defective strains.

248 **LbcA enhances CtpA-dependent degradation of MepM *in vitro*.** To test if
249 MepM is a direct substrate of CtpA, we purified C-terminal hexahistidine tagged
250 proteins. MepM was stable when incubated alone, but in the presence of CtpA the
251 amount of MepM decreased (Fig. 7A). Furthermore, when MepM was incubated with
252 both CtpA and LbcA it became undetectable, which is consistent with LbcA enhancing
253 CtpA-dependent degradation (Fig. 7A). There was no MepM degradation when it was
254 incubated with CtpA-S302A +/- LbcA. This supports the contentions that the S302A

255 mutation destroys CtpA activity, that MepM degradation was due to CtpA and not a
256 contaminating protease activity, and that LbcA cannot degrade MepM itself.

257 We also monitored the CtpA-dependent degradation of MepM over time and
258 found that it was faster in the presence of LbcA (Fig. 7B). Finally, we incubated CtpA
259 with another LytM/M23 peptidase domain protein, PA3787. However, PA3787 was not
260 degraded significantly, showing that CtpA has substrate specificity (Fig. 7B). These *in*
261 *vitro* experiments support the characterization of MepM as a direct substrate of CtpA
262 and suggest that LbcA catalyzes the proteolysis.

263 **The LbcA•CtpA complex degrades additional peptidoglycan cross-link**
264 **hydrolases.** MepM was the most abundant protein co-purified with LbcA•CtpA-S302A.
265 Remarkably, the three proteins with the next highest PSMs are also known or predicted
266 peptidoglycan hydrolases (PA1198, MltD and RlpA; Fig. 4B). PA1198 is homologous to
267 *E. coli* NlpC/P60 peptidase family member MepS, a DD-endopeptidase that targets the
268 same peptidoglycan cross-links as MepM (23). MltD and RlpA are lytic
269 transglycosylases that attack the glycan chain (38-40).

270 To test if CtpA might cleave these putative peptidoglycan hydrolases, we
271 constructed plasmids encoding arabinose inducible FLAG tagged versions. PA1198-
272 FLAG was undetectable in the wild type, whereas it became abundant in a $\Delta ctpA$
273 mutant (Fig. 8A). We extended the PA1198 analysis to an $\Delta lbcA$ mutant, in which it also
274 accumulated (Fig. 8A). Therefore, PA1198 might also be an LbcA•CtpA substrate.
275 However, MltD-FLAG and RlpA-FLAG were detectible in wild type strains and did not
276 accumulate in a $\Delta ctpA$ mutant (Fig. 8A). This suggests that MltD and RlpA are not CtpA
277 substrates (see Discussion).

278 We also used a biased approach by screening some putative *P. aeruginosa*
279 peptidoglycan hydrolases. Again, this was done by constructing plasmids encoding
280 arabinose inducible FLAG tagged versions. Candidates included three members of the
281 LytM/M23 peptidase family that MepM is in (PA3787, PA4404 and PA5551), two
282 members of the LytM/M23 family with predicted defective peptidase domains
283 (PA3623/NlpD and PA5363), and three members of the NlpC/P60 family that PA1198 is
284 in (PA0639, PA1199 and PA1844/Tse1). We also tested PA2272 (PBP3A) and PA4418
285 (PBP3), two homologs of *E. coli* penicillin binding protein 3 (PBP3/FtsI), which has been
286 proposed to be proteolytically processed by its CTP, Prc/Tsp (8). Most of these
287 candidates did not accumulate in a $\Delta ctpA$ mutant, suggesting that they are not
288 substrates (Fig 8A). However, PA1199 and PA4404 were not detected in wild type but
289 accumulated in the $\Delta ctpA$ mutant. We extended their analysis to an $\Delta lbcA$ mutant, in
290 which they also accumulated (Fig. 8A). Therefore, PA1199 and PA4404 are also
291 putative LbcA•CtpA proteolytic substrates.

292 To confirm PA1198, PA1199 and PA4404 as CtpA substrates, we purified
293 hexahistidine tagged versions and tested them *in vitro*. All were degraded when
294 incubated with LbcA and CtpA, but there was no degradation by CtpA-S302A (Fig. 8B).
295 Therefore, CtpA degrades two peptidoglycan hydrolases in the LytM/M23 peptidase
296 family (MepM and PA4404), and two in the NlpC/P60 family (PA1198 and PA1199).
297 Their sequences predict all to be in the cell envelope, MepM as a peptidoglycan-
298 associated protein and PA1198, PA1199 and PA4404 as outer membrane lipoproteins.
299 Furthermore, all are predicted to cleave the peptide cross-links of peptidoglycan.
300 Breaking these cross-links poses a danger to the bacterial cell and the LbcA•CtpA

301 complex might be an important control mechanism used by *P. aeruginosa* to regulate
302 this activity.

303 **LbcA•CtpA defective strains grow poorly in salt-free medium.** *E. coli prc*
304 mutants have altered cell morphology, and increased sensitivity to some drugs and low
305 osmolarity (20). Biolog Phenotype Microarray analysis of a *P. aeruginosa* $\Delta ctpA$ mutant
306 revealed no increased drug sensitivity (18). We have examined cells by light microscopy
307 after growth at 37°C or 42°C, in media with or without salt, and in exponential and
308 stationary phase, but $\Delta ctpA$ and $\Delta lbcA$ mutations did not noticeably affect cell shape or
309 length (data not shown). This is not surprising because Prc and CtpA have different
310 substrates (Prc processes FtsI, which might contribute to filamentation of Δprc cells,
311 whereas CtpA does not appear to process *P. aeruginosa* FtsI homologs, Fig. 8A). Also,
312 *P. aeruginosa* has another CTP (PA3257/AlgO) that is a closer homolog of *E. coli* Prc
313 than is CtpA. Even so, if multiple peptidoglycan hydrolases accumulate in $\Delta ctpA/\Delta lbcA$
314 mutants (Fig. 8A), and peptidoglycan cross-linking is compromised (Fig. 6), then
315 sensitivity to low osmolarity is expected. Therefore, we also investigated this possibility.

316 $\Delta ctpA$ and $\Delta lbcA$ mutants grew more slowly than wild type in LB broth without
317 NaCl (Fig. 8C). This phenotype was not exacerbated at 42°C and/or on agar (data not
318 shown). Regardless, the occurrence and subtle nature of this phenotype is consistent
319 with the slightly reduced peptidoglycan cross-linking efficiency (Fig. 6). Importantly, this
320 phenotype was not fully suppressed by a $\Delta mepM$ mutation, which further supports
321 LbcA•CtpA degrading multiple peptidoglycan hydrolases.

322

323

324 **DISCUSSION**

325 We have discovered that *P. aeruginosa* CtpA forms a complex with LbcA, and
326 both proteins are required for CtpA-mediated proteolysis *in vivo* and *in vitro*. We
327 identified four proteolytic substrates, all of which are predicted to cleave the cross-links
328 between peptidoglycan chains. Therefore, the LbcA•CtpA complex might be an
329 important control mechanism used by *P. aeruginosa* to regulate peptidoglycan cross-
330 link hydrolysis. It has been difficult to investigate if substrate degradation is regulated,
331 because they are difficult to detect in protease-competent strains (e.g. Figs. 4 and 8).
332 However, even though CtpA and LbcA protein levels appear constant regardless of
333 growth stage, our preliminary evidence suggests that at least one substrate might be
334 degraded at different rates (D. Srivastava and A. J. Darwin, unpublished data).
335 Investigating how this occurs, and the signal(s) involved, are intriguing future questions.

336 An exciting parallel exists between the complex we have discovered, and the
337 Nlpl•Prc complex in *E. coli*. Prc is a CTP, and Nlpl is an outer membrane lipoprotein
338 with TPR motifs, and together they degrade one peptidoglycan hydrolase, MepS (22).
339 The similarities to LbcA•CtpA are obvious. However, Prc and CtpA are evolutionarily
340 divergent, differing in size by approximately 30 kDa and belonging to different CTP
341 subfamilies. Although Nlpl and LbcA are both outer membrane lipoproteins containing
342 short TPR motifs, their primary sequences are not similar and LbcA is much larger than
343 Nlpl. In the *E. coli* Nlpl•Prc complex, an Nlpl homodimer binds two Prc monomers to
344 create docking sites for the MepS substrate (41). The LbcA•CtpA complex in *P.*
345 *aeruginosa* could have similarities to this, but we suspect that its stoichiometry and
346 functioning will have differences, due to the divergence of the proteins involved.

347 Regardless, it is important that two very different CTPs, and two very different
348 lipoproteins, form complexes in two divergent bacterial species to degrade
349 peptidoglycan hydrolases. This suggests that this could be a widespread phenomenon
350 and a new paradigm might emerge in which many bacterial CTPs work with partner
351 proteins to target cell wall hydrolases.

352 LbcA•CtpA degrades four predicted peptidoglycan cross-link hydrolases (Figs. 4,
353 7-9). Consistent with this, a $\Delta ctpA$ mutant has a cell envelope structural defect when
354 viewed by electron microscopy (18), peptidoglycan cross-linking is reduced (Fig. 6), and
355 it grows poorly in LB broth without NaCl (Fig. 8C). All of this suggests a weakened cell
356 wall caused by increased peptidoglycan cross-link hydrolase activity. Removing the
357 MepM substrate did not suppress the slow growth of $\Delta ctpA$ and $\Delta lbcA$ mutants in salt
358 free medium (Fig. 8C). This indicates that at least one other CtpA substrate must
359 contribute to this phenotype. In fact, although it is not obvious from the growth curves,
360 the $\Delta mepM$ mutation did improve growth very slightly. Therefore, we hypothesize that
361 the poor growth in LB broth without NaCl results from the combined effect on the cell
362 wall of two or more accumulating CtpA substrates. We have not yet been able to make
363 null mutants of the other CtpA substrates, but a future goal is to investigate their roles.

364 The defective T3SS and accelerated surface attachment phenotypes of a $\Delta ctpA$
365 mutant are most likely to be secondary consequences of a compromised cell wall.
366 However, these phenotypes were efficiently suppressed by a $\Delta mepM$ mutation. MepM
367 was the most abundant protein trapped by the LbcA•CtpA-S302A complex (Fig. 4B) and
368 so it might be having the largest influence on the cell wall. If so, even though removing
369 MepM might not fix all the cell wall problems, it might improve things sufficiently to

370 prevent effects on the T3SS and surface attachment. However, another possibility is
371 that MepM plays a more specialized role. In this regard it is intriguing to note that the
372 assembly of transenvelope systems, including a T3SS, requires rearrangement of the
373 peptidoglycan (42-44). Some T3SS-encoding loci encode a peptidoglycan hydrolase
374 that is needed for T3SS function (45, 46). Unlike MepM, these are lytic
375 transglycosylases, but it is still possible that a specific role of MepM is important for
376 T3SS assembly or function in *P. aeruginosa*. Indeed, many T3SS loci do not encode a
377 dedicated peptidoglycan hydrolase, raising the possibility that they rely on endogenous
378 cellular hydrolase(s). It is also worth noting the possibility that some peptidoglycan
379 hydrolases function in a complex and removing one of them destroys the function of the
380 entire complex. The lytic transglycosylases MltD and RlpA were pulled down by the
381 LbcA•CtpA-S302A trap, but they do not appear to be CtpA substrates (Figs 4B and 8A).
382 This could be explained by an interaction with a CtpA substrate such as MepM.

383 The MepM and PA4404 substrates are in the LytM/M23 family of peptidases, and
384 both have homology to *E. coli* MepM. However, indirect genetic evidence suggests that
385 Prc, the only CTP in *E. coli*, might not degrade MepM in that species (47). *E. coli* Prc
386 does degrade the NlpC/P60 peptidase family member MepS (22). This is notable,
387 because the CtpA substrates PA1198 and PA1199 are both homologous to *E. coli*
388 MepS. Therefore, despite being from divergent CTP subfamilies, *P. aeruginosa* CtpA
389 and *E. coli* Prc both degrade MepS-like hydrolases. This is surprising because *P.*
390 *aeruginosa* has a second CTP, and the other one is a homolog of *E. coli* Prc (PA3257,
391 also known as AlgO). The abundance of PA1198 and PA1199 in a $\Delta ctpA$ strain (Fig.
392 8A) suggests that Prc might not degrade MepS hydrolases in *P. aeruginosa*.

393 *P. aeruginosa* Prc was proposed to cleave the antisigma factor MucA, inducing
394 the extracytoplasmic function (ECF) sigma factor AlgT/U and alginate production (26-
395 28). However, the AlgT/U regulon can also be induced by cell wall-inhibitory antibiotics
396 (28). Therefore, it is possible that *P. aeruginosa* Prc cleaves one or more peptidoglycan
397 modifying enzymes, and its impact on the AlgT/U regulon is a consequence of altered
398 peptidoglycan rather than Prc cleaving MucA directly. In fact, CtpA overproduction
399 induces an ECF sigma factor that can be activated by the cell wall-inhibitory antibiotic
400 D-cycloserine, but CtpA is unlikely to cleave its antisigma factor (18). Prc has also been
401 implicated in activating several other ECF sigma factors in *Pseudomonas* species (48).
402 However, induction of ECF sigma factors by cell wall stress is common, and an effect of
403 Prc on peptidoglycan could perhaps be the explanation. Importantly, Prc has not been
404 shown to cleave any antisigma factor directly.

405 In summary, a binary protein complex degrades at least four proteins predicted to
406 cleave peptidoglycan cross-links in *P. aeruginosa* (Fig. 9). Therefore, LbcA•CtpA might
407 be an important mechanism used to control peptidoglycan hydrolysis, a reaction with
408 the potential for catastrophic consequences if it is not carefully constrained. Importantly,
409 similarities to the distantly related Nlpl•Prc system of *E. coli* suggest that this might be a
410 widespread phenomenon in diverse bacteria.

411

412

413 **MATERIALS AND METHODS**

414 **Bacterial strains and standard growth conditions.** Strains and plasmids are
415 listed in Table 1. Bacteria were grown routinely in Luria-Bertani (LB) broth or on LB agar

416 at 37°C. During conjugation procedures, *P. aeruginosa* was occasionally selected on
417 Vogel-Bonner minimal (VBM) agar. *E. coli* K-12 strain SM10 was used to conjugate
418 plasmids into *P. aeruginosa* (49).

419 **Plasmid and strain constructions.** To construct in frame deletion mutants, two
420 fragments of ~ 0.5 kb each corresponding to regions upstream and downstream of the
421 deletion site were amplified by PCR and cloned into pEX18Ap. The plasmids were
422 integrated into the *P. aeruginosa* chromosome after conjugation from *E. coli* and
423 sucrose resistant, carbenicillin sensitive segregants were isolated on LB agar containing
424 10% sucrose. Deletions were verified by colony PCR. $\Delta lbcA::aacC1$ mutants were
425 constructed similarly, except the *aacC1* cassette from plasmid p34s-Gm was cloned
426 between the upstream and downstream fragments in pEX18Ap.

427 To make strain AJDP1140 encoding CtpA-S302A, two ~ 0.5 kb fragments
428 flanking codon 302 of *ctpA* were amplified by PCR chromosome. For each fragment one
429 of the primers incorporated a mismatch at codon 302 to convert it to encode alanine.
430 The fragments were joined in a PCR SOEing reaction (50) via their overlapping regions
431 around codon 302. The product was cloned into pEX18Ap and exchanged for the
432 corresponding region of the *ctpA* gene by integration, selection for sucrose-resistant
433 segregants and confirmation by colony PCR and DNA-sequencing.

434 To make strains encoding CtpA-FLAG-His₆ and CtpA-S302A-FLAG-His₆, two ~
435 500 bp fragments surrounding the stop codon of *ctpA* were amplified by PCR. For each
436 fragment one primer incorporated a region encoding FLAG-His₆. The fragments were
437 joined in a PCR SOEing reaction via their overlapping FLAG-His₆ sequences. The
438 products were cloned into plasmid pEX18Ap and used to fuse the FLAG-His₆ encoding

439 region to the *ctpA* gene by integration, selection for sucrose-resistant segregants and
440 confirmation by colony PCR and DNA-sequencing.

441 Plasmids encoding C-terminal FLAG-tagged proteins were constructed by
442 amplifying genes using a downstream primer that incorporated a region encoding the
443 FLAG tag, and then cloning into pHERD20T or pVLT35. Plasmids for protein
444 overproduction and purification were constructed by PCR amplification of genes, without
445 their predicted N-terminal signal sequences and stop codons, and cloning into pET-
446 24b(+) to encode C-terminal His₆-tagged versions.

447 **Polyclonal antiserum production and immunoblotting.** *E. coli* strain ER2566
448 (NEB) containing a pET-24b(+) derivative encoding MepM-His₆, LbcA-His₆ or OprF-His₆
449 was grown in LB broth to mid-log phase at 37°C with aeration. Protein production was
450 induced with 1mM IPTG for 4 hrs at 37°C for LbcA-His₆ and OprF-His₆, or overnight at
451 16°C for MepM-His₆. Proteins were purified under denaturing conditions by nickel-
452 nitrilotriacetic acid (NTA) affinity chromatography as described by the manufacturer
453 (Qiagen). Polyclonal rabbit antisera were raised by Covance Research Products Inc.

454 Semi dry electroblotting was used to transfer SDS-PAGE separated samples to
455 nitrocellulose. Chemiluminescent detection followed incubation with polyclonal
456 antiserum or monoclonal antibody, then goat anti-rabbit IgG (Sigma) or goat anti-mouse
457 IgG (Sigma) horseradish peroxidase conjugates used at the manufacturers
458 recommended dilution. Primary antisera or antibodies were diluted 5,000-fold for anti-
459 THE-His (GenScript) and anti-FLAG M2 (Sigma), 7,500-fold for anti-MepM, 8,000-fold
460 for anti-LbcA, 10,000-fold for anti-PA0943, anti-PA4068 and anti-CtpA (18, 51) and
461 20,000 fold for anti-OprF.

462 **CtpA-FLAG-His₆ tandem purification.** Strains were grown in 100 ml LB broth at
463 37°C with aeration to OD 600 nm ~ 1.2 - 1.4 and cells were collected by centrifugation.
464 For formaldehyde cross-linking, the pellet was washed with cold 10 mM potassium
465 phosphate buffer pH 8.0 and resuspended to an OD 600 nm of 5 in the same buffer. 1%
466 formaldehyde was added followed by incubation at room temperature for 30 min. 0.3 M
467 Tris-HCl pH 7.5 was added to quench and the cells were collected by centrifugation.
468 Pellets were resuspended in 3 ml lysis buffer (50 mM Tris-HCl pH 7.5, 150 mM NaCl, 5
469 mM Imidazole), and Roche complete protease inhibitors (2x concentration), 1 µg/ml
470 DNaseI, 1 µg/ml RNase, and 1 mg/ml lysozyme were added. Cells were disrupted by
471 sonication, then 1% *n*-dodecyl β-D-maltoside (DDM) was added followed by incubation
472 with rotation for 30 min at 4°C. Insoluble material was removed by centrifugation at
473 13,000 x *g* for 30 min at 4°C. 200 µl of nickel-NTA agarose in lysis buffer was added to
474 the supernatant, followed by incubation with rotation for 1.5 h at 4°C. The resin was
475 collected in a drip column and washed with 4 ml lysis buffer, then 4 ml lysis buffer
476 containing 20 mM imidazole. Proteins were eluted in 1 ml lysis buffer containing 250
477 mM imidazole, mixed with 30 µl anti-FLAG M2 agarose resin (Sigma) in TBS (10 mM
478 Tris-HCl pH 7.5, 150 mM NaCl), and incubated with rotation for 2 h at 4°C. A 1 ml spin
479 column (Pierce 69725) was used to wash the resin three times with 800 µl TBS.
480 Proteins were eluted by adding 100 µl of 2 µg/ml FLAG peptide (F3290 Sigma) in TBS
481 and incubating with rotation at 4°C for 30 min. Proteins were identified by LC-mass
482 spectrometry (NYU School of Medicine Proteomics Laboratory).

483 **CtpA-His₆, LbcA-FLAG tandem purification.** Δ *ctpA* strains containing pVLT35
484 derivatives encoding CtpA-His₆ or CtpA-S302A-His₆, and pHERD20T encoding LbcA-

485 FLAG, were inoculated to an OD 600 nm of 0.05 in 250 ml LB broth containing 5 mM
486 EGTA, 100 μ M IPTG and 0.02% (w/v) arabinose. Cultures were incubated at 37°C with
487 225 rpm rotation until the OD 600 nm was \sim 1.5. Procedures described in the preceding
488 section were used for protein purification and identification.

489 **Analysis of T3SS substrates in cell free supernatants.** Strains were
490 inoculated at OD 600 nm of 0.04 in test tubes containing 5 ml Tryptic Soy Broth (TSB)
491 containing 5 mM EGTA, and grown for 6 h at 37°C on a roller. Cells from the equivalent
492 of 1 ml of culture at OD 600 nm of 1.5 were removed by centrifugation at 3,300 x g for
493 15 min at 4°C. The supernatant was filtered with a 0.22 μ m filter, then 1/10th volume
494 trichloroacetic acid was added, followed by incubation at 4°C overnight. Proteins were
495 collected by centrifugation at 4,500 x g for 40 min at 4°C, washed twice with 1 ml ice
496 cold acetone, dried at room temperature for 30-40 min, and resuspended in SDS-PAGE
497 sample buffer. Proteins were separated by SDS PAGE and stained with silver.

498 **Surface attachment.** Saturated cultures in LB broth were diluted to an OD 600
499 nm of 0.1 in 13 x 100 mm borosilicate glass tubes containing 0.5 ml of M63 salts
500 supplemented with 1 mM MgSO₄, 0.5% (w/v) casamino acids and 0.2% (w/v) glucose.
501 The tubes were incubated at 30°C without agitation for 8 h. Culture medium was
502 removed and the tubes were washed twice with 2 ml of water. 500 μ l of 0.1% (w/v)
503 crystal violet was added followed by incubation at room temperature for 10 min, two
504 washes with 10 ml water, and then the tubes were inverted for 10 min at room
505 temperature and photographed. The crystal violet was dissolved in 1 ml ethanol and
506 absorbance at 595 nm was measured. A tube that contained growth medium alone was
507 used to generate the blank.

508 **Subcellular fractionation.** Osmotic shock was done as previously (18), except
509 that cultures were grown to OD 600 nm of ~ 1. To generate soluble and insoluble
510 fractions, 100 ml cultures in LB broth were grown at 37°C with shaking at 225 rpm to an
511 OD 600 nm of ~ 1. Cells were collected by centrifugation, washed with 10 ml of 20 mM
512 Tris-HCl pH 7.5, 20 mM EDTA (TE), resuspended in 10 ml cold TE containing Roche
513 complete protease inhibitors, and lysed by two passages through a French pressure cell
514 (1,100 psi). Intact cells were removed by centrifugation at 8,000 x *g* for 10 min at 4°C.
515 The supernatant was centrifuged at 100,000 x *g* for 1 h at 4°C. The supernatant was the
516 soluble fraction. The pellet (membrane fraction) was washed twice with 20 mM Tris-HCl
517 pH 7.5, and resuspended in 20 mM Tris-HCl pH 7.5 containing Roche complete
518 protease inhibitors.

519 **CHO-K1 cell cytotoxicity.** Chinese hamster ovary cells were grown in Roswell
520 Park Memorial Institute (RPMI) 1640 medium with 10% fetal bovine serum (FBS) and 2
521 mM glutamine, at 37°C in a 5% CO₂ atmosphere. 2x10⁵ cells/well were seeded in a 24-
522 well plate and incubated at 37°C for 16 h. Attached cells were washed with phosphate
523 buffered saline (PBS) and covered with RPMI 1640 containing 1% FBS and 2 mM
524 glutamine. *P. aeruginosa* was grown in TSB at 37°C until the OD 600 nm was 0.8, then
525 added to the CHO-K1 cells at a multiplicity of infection of ~ 10. The plate was
526 centrifuged at 250 x *g* for 5 min and incubated for 4 h at 37°C. Supernatants were
527 collected after centrifugation at 250 x *g* for 5 min and lactate dehydrogenase (LDH)
528 concentration was measured with the LDH Cytotox assay (Promega).

529 **Cell wall isolation and digestion.** Bacteria were grown to saturation in 500 ml
530 LB broth at 37 °C with 150 rpm shaking. Cells were harvested by centrifuging at 5,200 x

531 g for 20 min, resuspended in PBS, and sterilized by boiling for 60 min. Samples were
532 bead beaten (Bead Mill 24; Fisher Scientific) with 0.5 mm diameter glass beads for ten 1
533 min cycles with 1 min rests. Beads were removed using a Steriflip 20 μ m nylon vacuum
534 filter (EMD Millipore). Crude cell wall pellets were resuspended in 2 ml PBS, to which
535 8 ml of 2% SDS (w/v) was added. They were boiled for 60 min, washed with deionized
536 water, and resuspended in 2 ml of 50 mM Tris pH 8.0. 200 μ g DNase was added and
537 incubated at 37 °C for 24 h and 150 rpm, followed by 200 μ g pronase E and another
538 24 h incubation. Cell walls were washed once and resuspended in 1 ml of 50 mM Tris
539 pH 8.0, then digested by adding 0.5 KU of mutanolysin (Sigma-Aldrich) and incubating
540 at room temperature for 24 h. Another 0.5 KU of mutanolysin was added followed by
541 another 24 h incubation. Digested cell walls were frozen, lyophilized, and dissolved in
542 1 ml of 0.375 M sodium borate buffer (pH 9.0) using HPLC-grade water. Muropeptides
543 were reduced by adding 10 mg of sodium borohydride at room temperature for 30 min.
544 Reduction was quenched by adding 125 μ l phosphoric acid. Samples were frozen at -
545 80 °C, lyophilized, resuspended in 1 ml of 1% trifluoroacetic acid, centrifuge filtered, and
546 cleaned up for LC-MS using 100 μ l Pierce C18 tips.

547 **Peptidoglycan analysis by liquid chromatography-mass spectrometry.**
548 Mutanolysin-digested muropeptide fragments were separated using a NanoACQUITY
549 Ultra Performance Liquid Chromatography System (Waters). A reverse phase BEH C18
550 column (length 100 mm, diameter 75 μ m) of 1.7 μ m bead with pore size of 130 Å was
551 used. Separation was carried out by injecting 2 μ l of mutanolysin-digested PG from a
552 5 μ l sample loop to the column under isocratic condition of 98% mobile phase A (0.1%
553 formic acid in HPLC water) and 2% mobile phase B (90% acetonitrile & 10% of HPLC

554 water added with 0.1% formic acid) for 5 min, then a linear gradient to 50% buffer B was
555 applied for 30 min. The column was regenerated under isocratic condition with 85%
556 buffer B for 5 min, a linear gradient to 98% buffer A for 1 min, then isocratic at 98%
557 buffer A for 23 min. The flow rate was kept constant (0.6 μ l/min) throughout the analysis.
558 Fibrinopeptide B (Glu-Fib) was used as an internal standard. Data were analyzed using
559 MassLynx (Waters) and MATLAB (MathWorks).

560 ***In vitro* proteolysis.** *E. coli* ER2566 (NEB) containing each pET-24b(+)
561 derivative were grown in 1L LB broth at 37°C with aeration until the OD 600 nm was 0.6-
562 0.8. Protein production was induced by adding 1 mM IPTG and incubating for 16 h at
563 16°C with aeration. Proteins were purified under native conditions by NTA agarose
564 affinity chromatography as recommended by the manufacturer (Qiagen). Following
565 elution with imidazole, proteins were exchanged into 50 mM NaH₂PO₄, 300 mM NaCl pH
566 8.0, using Amicon Ultra-4 centrifuge filter devices (10 kDa cutoff), then supplemented
567 with 10% glycerol and stored at -20°C. However, CtpA-His₆ and CtpA-S302A-His₆ only
568 were eluted sequentially with 50 mM NaH₂PO₄, 300 mM NaCl, pH 8.0, containing 50
569 mM, 100 mM, 150 mM, 200 mM or 250 mM imidazole. Buffer exchange and freezing
570 was not possible due to precipitation. Therefore, CtpA-His₆ and CtpA-S302A-His₆ were
571 purified, stored at 4°C, and used within 48 h. All experiments were done at least three
572 times with representative experiments shown in the figures.

573 **Growth curves.** Saturated cultures were diluted into 5 ml of LB broth, containing
574 either 1% (w/v) NaCl or no NaCl, in 18 mm diameter test tubes so that the initial OD 600
575 nm was approximately 0.1. The cultures were grown on a roller drum at 37°C for 9 h
576 and 0.1 ml samples were removed at hourly intervals for OD 600 nm measurement.

577

578 **ACKNOWLEDGEMENTS**

579 We thank Sindhoora Singh for constructing plasmid pAJD2003. Research was
580 supported by the National Institute of Allergy and Infectious Diseases (NIAID) of the
581 National Institutes of Health, under Award Numbers R21AI117131 and R01AI136901.
582 The content is solely the responsibility of the authors and does not necessarily
583 represent the official views of the National Institutes of Health. Mass spectrometric
584 protein identification done by NYU School of Medicine's proteomics laboratory was
585 partly supported by NYU School of Medicine. S.J.K. and B.R. conducted the
586 peptidoglycan analysis and analyzed the data, were supported by the National Institutes
587 of Health Grant GM116130, and acknowledge the Baylor University Mass Spectrometry
588 Centre (BU-MS) for support.

589

590 **REFERENCES**

- 591 1. Driscoll JA, Brody SL, Kollef MH. 2007. The epidemiology, pathogenesis and
592 treatment of *Pseudomonas aeruginosa* infections. *Drugs* 67:351-368.
- 593 2. Hauser AR. 2009. The type III secretion system of *Pseudomonas aeruginosa*:
594 infection by injection. *Nat Rev Microbiol* 7:654-665.
- 595 3. Wagner VE, Iglewski BH. 2008. *P. aeruginosa* Biofilms in CF Infection. *Clin Rev*
596 *Allergy Immunol* 35:124-134.
- 597 4. Clark ST, Diaz Caballero J, Cheang M, Coburn B, Wang PW, Donaldson SL, Zhang
598 Y, Liu M, Keshavjee S, Yau YCW, Waters VJ, Elizabeth Tullis D, Guttman DS,
599 Hwang DM. 2015. Phenotypic diversity within a *Pseudomonas aeruginosa*
600 population infecting an adult with cystic fibrosis. *Sci Rep* 5:10932.
- 601 5. Moore NM, Flaws ML. 2011. Epidemiology and pathogenesis of *Pseudomonas*
602 *aeruginosa* infections. *Clin Lab Sci* 24:43-46.
- 603 6. Lyczak JB, Cannon CL, Pier GB. 2000. Establishment of *Pseudomonas aeruginosa*
604 infection: lessons from a versatile opportunist. *Microbes Infect* 2:1051-1060.
- 605 7. Rawlings ND, Barrett AJ, Bateman A. 2010. MEROPS: the peptidase database.
606 *Nucleic Acids Res* 38:D227-233.
- 607 8. Hara H, Yamamoto Y, Higashitani A, Suzuki H, Nishimura Y. 1991. Cloning,
608 mapping, and characterization of the *Escherichia coli* *prc* gene, which is involved in
609 C-terminal processing of penicillin-binding protein 3. *J Bacteriol* 173:4799-4813.
- 610 9. Keiler KC, Silber KR, Downard KM, Papayannopoulos IA, Biemann K, Sauer RT.
611 1995. C-terminal specific protein degradation: activity and substrate specificity of the
612 Tsp protease. *Protein Sci* 4:1507-1515.

- 613 10. Che Y, Fu A, Hou X, McDonald K, Buchanan BB, Huang W, Luan S. 2013. C-
614 terminal processing of reaction center protein D1 is essential for the function and
615 assembly of photosystem II in *Arabidopsis*. Proc Natl Acad Sci USA 110:16247-
616 16252.
- 617 11. Satoh K, Yamamoto Y. 2007. The carboxyl-terminal processing of precursor D1
618 protein of the photosystem II reaction center. Photosynth Res 94:203-215.
- 619 12. Kumru OS, Bunikis I, Sorokina I, Bergstrom S, Zuckert WR. 2011. Specificity and
620 role of the *Borrelia burgdorferi* CtpA protease in outer membrane protein
621 processing. J Bacteriol 193:5759-5765.
- 622 13. Bandara AB, DeShazer D, Inzana TJ, Sriranganathan N, Schurig GG, Boyle SM.
623 2008. A disruption of *ctpA* encoding carboxy-terminal protease attenuates
624 *Burkholderia mallei* and induces partial protection in CD1 mice. Microb Pathog
625 45:207-216.
- 626 14. Bandara AB, Sriranganathan N, Schurig GG, Boyle SM. 2005. Carboxyl-terminal
627 protease regulates *Brucella suis* morphology in culture and persistence in
628 macrophages and mice. J Bacteriol 187:5767-5775.
- 629 15. Carroll RK, Rivera FE, Cavaco CK, Johnson GM, Martin D, Shaw LN. 2014. The
630 lone S41 family C-terminal processing protease in *Staphylococcus aureus* is
631 localized to the cell wall and contributes to virulence. Microbiology 160:1737-1748.
- 632 16. Deng CY, Deng AH, Sun ST, Wang L, Wu J, Wu Y, Chen XY, Fang RX, Wen TY,
633 Qian W. 2014. The periplasmic PDZ domain-containing protein Prc modulates full
634 virulence, envelopes stress responses, and directly interacts with dipeptidyl

- 635 peptidase of *Xanthomonas oryzae* pv. *oryzae*. Mol Plant Microbe Interact 27:101-
636 112.
- 637 17. Mitchell SJ, Minnick MF. 1997. A carboxy-terminal processing protease gene is
638 located immediately upstream of the invasion-associated locus from *Bartonella*
639 *bacilliformis*. Microbiology 143:1221-1233.
- 640 18. Seo J, Darwin AJ. 2013. The *Pseudomonas aeruginosa* periplasmic protease CtpA
641 can affect systems that impact its ability to mount both acute and chronic infections.
642 Infect Immun 81:4561-4570.
- 643 19. Lad SP, Yang G, Scott DA, Wang G, Nair P, Mathison J, Reddy VS, Li E. 2007.
644 Chlamydial CT441 is a PDZ domain-containing tail-specific protease that interferes
645 with the NF-kappaB pathway of immune response. J Bacteriol 189:6619-6625.
- 646 20. Seoane A, Sabbaj A, McMurry LM, Levy SB. 1992. Multiple antibiotic susceptibility
647 associated with inactivation of the *prc* gene. J Bacteriol 174:7844-7847.
- 648 21. Wang CY, Wang SW, Huang WC, Kim KS, Chang NS, Wang YH, Wu MH, Teng
649 CH. 2012. Prc contributes to *Escherichia coli* evasion of classical complement-
650 mediated serum killing. Infect Immun 80:3399-3409.
- 651 22. Singh SK, Parveen S, SaiSree L, Reddy M. 2015. Regulated proteolysis of a cross-
652 link-specific peptidoglycan hydrolase contributes to bacterial morphogenesis. Proc
653 Natl Acad Sci USA 112:10956-10961.
- 654 23. Singh SK, SaiSree L, Amrutha RN, Reddy M. 2012. Three redundant murein
655 endopeptidases catalyse an essential cleavage step in peptidoglycan synthesis of
656 *Escherichia coli* K12. Mol Microbiol 86:1036-1051.

- 657 24. Silber KR, Keiler KC, Sauer RT. 1992. Tsp: a tail-specific protease that selectively
658 degrades proteins with nonpolar C termini. *Proc Natl Acad Sci U S A* 89:295-299.
- 659 25. Keiler KC, Waller PR, Sauer RT. 1996. Role of a peptide tagging system in
660 degradation of proteins synthesized from damaged messenger RNA. *Science*
661 271:990-993.
- 662 26. Reiling SA, Jansen JA, Henley BJ, Singh S, Chattin C, Chandler M, Rowen DW.
663 2005. Prc protease promotes mucoidy in *mucA* mutants of *Pseudomonas*
664 *aeruginosa*. *Microbiology* 151:2251-2261.
- 665 27. Sautter R, Ramos D, Schneper L, Ciofu O, Wassermann T, Koh CL, Heydorn A,
666 Hentzer M, Hoiby N, Kharazmi A, Molin S, Devries CA, Ohman DE, Mathee K.
667 2012. A complex multilevel attack on *Pseudomonas aeruginosa algT/U* expression
668 and *algT/U* activity results in the loss of alginate production. *Gene* 498:242-253.
- 669 28. Wood LF, Leech AJ, Ohman DE. 2006. Cell wall-inhibitory antibiotics activate the
670 alginate biosynthesis operon in *Pseudomonas aeruginosa*: roles of σ^{22} (AlgT) and
671 the AlgW and Prc proteases. *Mol Microbiol* 62:412-426.
- 672 29. Hoge R, Laschinski M, Jaeger K-E, Wilhelm S, Rosenau F. 2011. The subcellular
673 localization of a C-terminal processing protease in *Pseudomonas aeruginosa*.
674 *FEMS Microbiol Lett* 316:23-30.
- 675 30. Yeung AT, Torfs EC, Jamshidi F, Bains M, Wiegand I, Hancock RE, Overhage J.
676 2009. Swarming of *Pseudomonas aeruginosa* is controlled by a broad spectrum of
677 transcriptional regulators, including MetR. *J Bacteriol* 191:5592-5602.
- 678 31. Blatch GL, Lässle M. 1999. The tetratricopeptide repeat: a structural motif mediating
679 protein-protein interactions. *Bioessays* 21:932-939.

- 680 32. Wurtzel O, Yoder-Himes DR, Han K, Dandekar AA, Edelheit S, Greenberg EP,
681 Sorek R, Lory S. 2012. The single-nucleotide resolution transcriptome of
682 *Pseudomonas aeruginosa* grown in body temperature. PLoS Pathog 8:e1002945.
- 683 33. O'Toole GA, Kolter R. 1998. Initiation of biofilm formation in *Pseudomonas*
684 *fluorescens* WCS365 proceeds via multiple, convergent signalling pathways: a
685 genetic analysis. Mol Microbiol 28:449-461.
- 686 34. Lee VT, Smith RS, Tümmler B, Lory S. 2005. Activities of *Pseudomonas aeruginosa*
687 effectors secreted by the type III secretion system in vitro and during infection. Infect
688 Immun 73:1695-1705.
- 689 35. Chang JD, Foster EE, Thadani AN, Ramirez AJ, Kim SJ. 2017. Inhibition of
690 *Staphylococcus aureus* cell wall biosynthesis by desleucyl-oritavancin: a quantitative
691 peptidoglycan composition analysis by mass spectrometry. J Bacteriol 199:e00278-
692 00217.
- 693 36. Chang JD, Foster EE, Wallace AG, Kim SJ. 2017. Peptidoglycan O-acetylation
694 increases in response to vancomycin treatment in vancomycin-resistant
695 *Enterococcus faecalis*. Sci Rep 7:46500.
- 696 37. Chang JD, Foster EE, Yang H, Kim SJ. 2017. Quantification of the d-Ala-d-Lac-
697 terminated peptidoglycan structure in vancomycin-resistant *Enterococcus faecalis*
698 using a combined solid-state nuclear magnetic resonance and mass spectrometry
699 analysis. Biochemistry 56:612-622.
- 700 38. Bateman A, Bycroft M. 2000. The structure of a LysM domain from *E. coli*
701 membrane-bound lytic murein transglycosylase D (MltD). J Mol Biol 299:1113-1119.

- 702 39. Lee M, Heseck D, Llarrull LI, Lastochkin E, Pi H, Boggess B, Mobashery S. 2013.
703 Reactions of all *Escherichia coli* lytic transglycosylases with bacterial cell wall. J Am
704 Chem Soc 135:3311-3314.
- 705 40. Jorgenson MA, Chen Y, Yahashiri A, Popham DL, Weiss DS. 2014. The bacterial
706 septal ring protein RlpA is a lytic transglycosylase that contributes to rod shape and
707 daughter cell separation in *Pseudomonas aeruginosa*. Mol Microbiol 93:113-128.
- 708 41. Su M-Y, Som N, Wu C-Y, Su S-C, Kuo Y-T, Ke L-C, Ho M-R, Tzeng S-R, Teng C-H,
709 Mengin-Lecreux D, Reddy M, Chang C-I. 2017. Structural basis of adaptor-
710 mediated protein degradation by the tail-specific PDZ-protease Prc. Nat Commun
711 8:1516.
- 712 42. Dijkstra AJ, Keck W. 1996. Peptidoglycan as a barrier to transenvelope transport. J
713 Bacteriol 178:5555-5562.
- 714 43. Koraimann G. 2003. Lytic transglycosylases in macromolecular transport systems of
715 Gram-negative bacteria. Cell Mol Life Sci 60:2371-2388.
- 716 44. Scheurwater EM, Burrows LL. 2011. Maintaining network security: how
717 macromolecular structures cross the peptidoglycan layer. FEMS Microbiol Lett
718 318:1-9.
- 719 45. Burkinshaw BJ, Deng W, Lameignere E, Wasney GA, Zhu H, Worrall LJ, Finlay BB,
720 Strynadka NC. 2015. Structural analysis of a specialized type III secretion system
721 peptidoglycan-cleaving enzyme. J Biol Chem 290:10406-10417.
- 722 46. Hausner J, Hartmann N, Jordan M, Buttner D. 2017. The predicted lytic
723 transglycosylase HpaH from *Xanthomonas campestris* pv. vesicatoria associates

- 724 with the type III secretion system and promotes effector protein translocation. Infect
725 Immun 85:pii: e00788-00716.
- 726 47. Lai GC, Cho H, Bernhardt TG. 2017. The mecillinam resistome reveals a role for
727 peptidoglycan endopeptidases in stimulating cell wall synthesis in *Escherichia coli*.
728 PLoS Genet 13:e1006934.
- 729 48. Bastiaansen KC, Ibañez A, Ramos JL, Bitter W, Llamas MA. 2014. The Prc and
730 RseP proteases control bacterial cell-surface signalling activity. Environ Microbiol
731 16:2433-2443.
- 732 49. Miller VL, Mekalanos JJ. 1988. A novel suicide vector and its use in construction of
733 insertion mutations: osmoregulation of outer membrane proteins and virulence
734 determinants in *Vibrio cholerae* requires *toxR*. J Bacteriol 170:2575-2583.
- 735 50. Heckman KL, Pease LR. 2007. Gene splicing and mutagenesis by PCR-driven
736 overlap extension. Nat Protoc 2:924-932.
- 737 51. Seo J, Brencic A, Darwin AJ. 2009. Analysis of secretin-induced stress in
738 *Pseudomonas aeruginosa* suggests prevention rather than response and identifies
739 a novel protein involved in secretin function. J Bacteriol 191:898-908.
- 740 52. Strom MS, Lory S. 1986. Cloning and expression of the pilin gene of *Pseudomonas*
741 *aeruginosa* PAK in *Escherichia coli*. J Bacteriol 165:367-372.
- 742 53. Qiu D, Damron FH, Mima T, Schweizer HP, Yu HD. 2008. PBAD-based shuttle
743 vectors for functional analysis of toxic and highly regulated genes in *Pseudomonas*
744 and *Burkholderia* spp. and other bacteria. Appl Environ Microbiol 74:7422-7426.
- 745 54. Hoang TT, Karkhoff-Schweizer RR, Kutchma AJ, Schweizer HP. 1998. A broad-
746 host-range Flp-FRT recombination system for site-specific excision of

- 747 chromosomally-located DNA sequences: application for isolation of unmarked
748 *Pseudomonas aeruginosa* mutants. Gene 212:77-86.
- 749 55. de Lorenzo V, Eltis L, Kessler B, Timmis KN. 1993. Analysis of *Pseudomonas* gene
750 products using *lacI^Δ/Ptrp-lac* plasmids and transposons that confer conditional
751 phenotypes. Gene 123:17-24.
- 752 56. Dennis JJ, Zylstra GJ. 1998. Plasposons: Modular self-cloning minitransposon
753 derivatives for rapid genetic analysis of Gram-negative bacterial genomes. Appl
754 Environ Microbiol 64:2710-2715.
- 755

756 **TABLE 1** Strains and plasmids

| 757 | Name | Genotype/Features | Reference or Source |
|-----|------------------------------|--|----------------------|
| 758 | <i>P. aeruginosa</i> strains | | |
| 759 | <i>P. aeruginosa</i> strains | | |
| 760 | PAK ^a | wild type strain | (52) |
| 761 | AJDP566 | <i>pscC::pAJD1</i> | (18) |
| 762 | AJDP730 | Δ <i>ctpA</i> | (18) |
| 763 | AJDP1091 | Δ <i>lbcA::aacC1</i> | This study |
| 764 | AJDP1133 | Φ [<i>ctpA-flag-his₆</i>] | This study |
| 765 | AJDP1140 | <i>ctpA-S302A</i> | This study |
| 766 | AJDP1153 | Φ [<i>ctpA-S302A-flag-his₆</i>] | This study |
| 767 | AJDP1228 | Δ <i>mepM</i> | This study |
| 768 | AJDP1229 | Δ <i>ctpA</i> Δ <i>mepM</i> | This study |
| 769 | AJDP1230 | Δ <i>lbcA::aacC1</i> Δ <i>mepM</i> | This study |
| 770 | Plasmids | | |
| 771 | Plasmids | | |
| 772 | pHERD20T | Amp ^r , pMB1 <i>ori</i> , <i>araBp</i> expression vector | (53) |
| 773 | pET-24b(+) | Kan ^r , pMB1 <i>ori</i> , <i>T7p</i> expression vector | Novagen |
| 774 | pEX18Ap | Amp ^r , pMB1 <i>ori</i> , <i>oriT</i> , <i>sacB</i> ⁺ | (54) |
| 775 | pVLT35 | Sm ^r , Sp ^r , RSF1010 <i>ori</i> , <i>tacp</i> expression vector | (55) |
| 776 | p34s-Gm | Ap ^r , <i>aacC1</i> ⁺ (Gm ^r), pUC <i>ori</i> | (56) |
| 777 | pAJD2290 | <i>T7p-ctpA-his₆</i> in pET-24b(+) | (18) |
| 778 | pAJD2003 | <i>T7p-oprF-his₆</i> in pET-24b(+) | This study |
| 779 | pAJD2350 | <i>tacp-ctpA-his₆</i> in pVLT35 | (Seo & Darwin, 2013) |

| | | | |
|-----|----------|---|----------------------|
| 780 | pAJD2351 | <i>tacp-ctpA-S302A-his₆</i> in pVLT35 | (Seo & Darwin, 2013) |
| 781 | pAJD2226 | <i>araBp-ctpA-his₆</i> in pHERD20T | (Seo & Darwin, 2013) |
| 782 | pAJD2227 | <i>araBp-ctpA-S302A-his₆</i> in pHERD20T | (Seo & Darwin, 2013) |
| 783 | pAJD2443 | <i>tacp-lbcA-flag</i> in pVLT35 | This study |
| 784 | pAJD2653 | <i>T7p-⁺lbcA-his₆</i> in pET-24b(+) | This study |
| 785 | pAJD2655 | <i>T7p-⁺ctpA-S302A-his₆</i> in pET-24b(+) | This study |
| 786 | pAJD2779 | <i>araBp-mepM-flag</i> in pHERD20T | This study |
| 787 | pAJD2801 | <i>araBp-PA3623-flag</i> in pHERD20T | This study |
| 788 | pAJD2809 | <i>T7p-⁺mepM-his₆</i> in pET-24b(+) | This study |
| 789 | pAJD2816 | <i>araBp-PA1812-flag</i> in pHERD20T | This study |
| 790 | pAJD2817 | <i>araBp-PA4404-flag</i> in pHERD20T | This study |
| 791 | pAJD2818 | <i>araBp-PA3787-flag</i> in pHERD20T | This study |
| 792 | pAJD2820 | <i>araBp-PA1198-flag</i> in pHERD20T | This study |
| 793 | pAJD2821 | <i>araBp-PA1199-flag</i> in pHERD20T | This study |
| 794 | pAJD2832 | <i>T7p-⁺PA1198-his₆</i> in pET-24b(+) | This study |
| 795 | pAJD2833 | <i>T7p-⁺PA3787-his₆</i> in pET-24b(+) | This study |
| 796 | pAJD2834 | <i>T7p-⁺PA4404-his₆</i> in pET-24b(+) | This study |
| 797 | pAJD2835 | <i>araBp-PA0639-flag</i> in pHERD20T | This study |
| 798 | pAJD2836 | <i>araBp-PA1844-flag</i> in pHERD20T | This study |
| 799 | pAJD2837 | <i>araBp-PA2272-flag</i> in pHERD20T | This study |
| 800 | pAJD2839 | <i>araBp-PA5363-flag</i> in pHERD20T | This study |
| 801 | pAJD2840 | <i>araBp-PA5551-flag</i> in pHERD20T | This study |
| 802 | pAJD2842 | <i>araBp-PA4418-flag</i> in pHERD20T | This study |

| | | | |
|-----|----------|---|------------|
| 803 | pAJD2844 | <i>T7p-PA1199-his₆</i> in pET-24b(+) | This study |
| 804 | pAJD2877 | <i>araBp-rlpA-flag</i> in pHERD20T | This study |

805

806 ^a All *P. aeruginosa* strains are derivatives of strain PAK

807 **Figure legends**

808

809 **FIG 1** Identification of the CtpA interaction partner PA4667/LbcA. (A) Tandem affinity
810 tag purification. Proteins were purified from detergent solubilized lysates of the wild type
811 strain (CtpA), or derivatives encoding CtpA-FLAG-His₆ or the proteolytically inactive
812 CtpA-S302A-FLAG-His₆. Purification was done with nickel agarose (Stage 1) followed
813 by anti-FLAG M2 agarose resin (Stage 2). Samples were separated on a 12.5% SDS
814 polyacrylamide gel, which was stained with silver. Molecular-mass-marker proteins
815 (kDa) are labeled on the right-hand side. (B) Immunoblot analysis of detergent
816 solubilized lysate, and Stage 1 and 2 purified samples, prepared as in panel A. LbcA
817 and CtpA were detected with polyclonal antisera. Strains in which CtpA or CtpA-S302A
818 were not tagged with FLAG-His₆ served as negative controls. Approximate positions of
819 molecular-mass-marker proteins (kDa) are indicated on the left-hand side.

820

821 **FIG 2** $\Delta ctpA$ and $\Delta lbcA$ mutants share common phenotypes. (A) T3SS function. Wild
822 type, $\Delta ctpA$ or $\Delta lbcA$ strains contained the *tac* promoter expression plasmid pVLT35
823 (vector), or derivatives encoding CtpA, CtpA-S302A or LbcA as indicated. TSB growth
824 medium contained 1mM EGTA to induce T3SS activity, and 10 μ M IPTG to induce the
825 *tac* promoter of the complementing plasmids. Cell free supernatants derived from
826 equivalent amounts of cells were separated on a SDS-PAGE gel, which was stained
827 with silver. The region with the abundant T3SS effectors ExoT and ExoS is shown. (B)
828 Surface attachment. The same strains as in panel A were incubated in glass test tubes
829 at 30°C without agitation for 8 hours. The growth medium contained 10 μ M IPTG to

830 induce the *tac* promoter of the complementing plasmids. Bacterial cells attached to the
831 glass at the air/liquid interface were stained with crystal violet (purple rings). The stain
832 was dissolved in ethanol and quantified by measuring absorbance at 595 nm. All strains
833 were tested in triplicate and error bars represent the standard deviation from the mean.

834

835 **FIG 3** LbcA promotes retention of CtpA in spheroplast and membrane fractions. (A)
836 Osmotic shock fractionation. Total cell lysate (whole cells), as well as spheroplast and
837 periplasm fractions generated by osmotic shock, were separated by SDS-PAGE,
838 transferred to nitrocellulose and proteins detected with polyclonal antisera. PA0943 is a
839 soluble periplasmic protein control, and PA4068 is a cytoplasmic spheroplast-retention
840 control (18). (B) Fractionation of lysed cells. Cells were lysed by two passages through
841 a French pressure cell and separated into soluble and insoluble (Membrane) fractions
842 by ultracentrifugation. Samples derived from equivalent amounts of cells were
843 separated by SDS PAGE, transferred to nitrocellulose, and proteins detected with
844 polyclonal antisera. PA0943 is a soluble protein control and OprF is an insoluble outer
845 membrane control.

846

847 **FIG 4** Identification of MepM as a putative substrate of the LbcA•CtpA proteolytic
848 complex. (A) Tandem affinity tag purification. Proteins were purified from detergent
849 solubilized lysates of $\Delta ctpA$ strains. All strains had a plasmid encoding LbcA-FLAG as
850 well as a second plasmid encoding untagged CtpA (negative control), CtpA-His₆ or the
851 proteolytically inactive CtpA-S302A-His₆. Purification was done with nickel agarose
852 followed by anti-FLAG M2 agarose resin. Samples were separated on a 12.5% SDS

853 polyacrylamide gel, which was stained with silver. Molecular-mass-marker proteins
854 (kDa) are labeled on the left-hand side. An irrelevant region of the gel between the
855 marker and sample lanes has been removed. (B) Scatter plot of proteins identified by
856 mass spectrometry after purification from strains encoding CtpA-S302A-His₆. Data are
857 the average peptide spectrum matches (PSM) and sequence coverage from duplicate
858 purifications from strains with CtpA-S302A-His₆. Each point represents a different
859 protein. All proteins plotted were detected in both of the LbcA•CtpA-S302A-His₆
860 purifications but neither of duplicate LbcA•CtpA-His₆ purifications. (C) Immunoblot
861 analysis of equivalent amounts of whole cell lysates of wild type, $\Delta ctpA$ and $\Delta lbcA$
862 strains. All strains contained an arabinose-inducible expression plasmid encoding
863 MepM-FLAG and were grown in media containing 0.2% (w/v) arabinose. Approximate
864 positions of molecular-mass-marker proteins (kDa) are indicated on the left-hand side.
865 MepM-FLAG was detected with anti-FLAG monoclonal antibodies and CtpA and LbcA
866 were detected with polyclonal antisera. (D) Detection of endogenous MepM.
867 Immunoblot analysis of equivalent amounts of whole cell lysates of wild type and $\Delta ctpA$
868 strains. Strains contained the *tac* promoter expression plasmid pVLT35 (-), or
869 derivatives encoding CtpA or CtpA-S302A as indicated. Approximate positions of
870 molecular-mass-marker proteins (kDa) are indicated on the left-hand side. MepM, CtpA
871 and LbcA were detected with polyclonal antisera.

872

873 **FIG 5** A *mepM* null mutation suppresses $\Delta ctpA$ phenotypes. (A) T3SS function. Wild
874 type, $\Delta mepM$, $\Delta ctpA$ or $\Delta ctpA \Delta mepM$ strains contained the *araBp* promoter expression
875 plasmid pHERD20T (vector), or a derivative encoding MepM as indicated. TSB growth

876 medium contained 1 mM EGTA to induce T3SS activity, and 0.02% arabinose to induce
877 the *araB* promoter of pHERD20T. Cell free supernatants derived from equivalent
878 amounts of cells were separated by SDS-PAGE gel, which was stained with silver. The
879 region with the abundant T3SS effectors ExoT and ExoS is shown. (B) Cytotoxicity to
880 CHO-K1 cells. Strains with the indicated genotypes were added to CHO-K1 cells at a
881 multiplicity of infection of ~10 and incubated for 4 h. Cell-free supernatants were then
882 analyzed for lactate dehydrogenase (LDH) content. The amount of LDH in the
883 supernatant following incubation with the wild type strain was set to 100% and the
884 values for the mutants are shown as the relative percentage. Data were averaged from
885 three independent experiments with the error bars showing the standard deviation from
886 the mean. (C) Surface attachment. The same strains from panel A were incubated in
887 glass test tubes at 30°C without agitation for 8 hours. The growth medium contained
888 0.02% arabinose to induce the *araB* promoter of the complementing plasmids. Bacterial
889 cells attached to the glass at the air liquid interface were stained with crystal violet
890 (purple rings). The stain was dissolved in ethanol and quantified by measuring
891 absorbance at 595nm. All strains were tested in triplicate and error bars represent the
892 standard deviation from the mean.

893

894 **FIG 6** Changes in peptidoglycan composition of a Δ *ctpA* mutant. (A) Chemical structure
895 of the peptidoglycan-repeat unit in *P. aeruginosa*. The disaccharide of the
896 peptidoglycan-repeat unit is shown with two modifications: O-acetylation of MurNAc at
897 C6 position and amidation of D-iso-Glu in the peptide stem to D-iso-Gln. The inter-
898 peptide bridge structure in *P. aeruginosa* is *m*-Dap. A schematic representation of a

899 peptidoglycan-repeat unit is shown as a figure inset with the disaccharide as gray-filled
900 circles, the amino acids in the pentapeptide stem as open triangles, and the inter-
901 peptide bridge structure as a line. The polymerized peptidoglycans are cross-linked by
902 forming a peptide bond between the sidechain of *m*-Dap from one repeat unit to the
903 carbonyl carbon of penultimate D-Ala of a peptidoglycan stem from a neighboring glycan
904 chain. (B) The mutanolysin-digested muropeptide fragments were characterized by LC-
905 MS. Forty-seven unique muropeptide ions from the wild type and thirty-three from the
906 $\Delta ctpA$ mutant were identified from LC-MS and each muropeptide was quantified by
907 integrating the extracted ion chromatogram (XIC) of the selected muropeptide ion.
908 Peptidoglycan dimers are the most abundant muropeptides found in both wild type and
909 $\Delta ctpA$ mutant with percent compositions of $87.30\% \pm 1.34\%$ and $75.85\% \pm 3.90\%$,
910 respectively. Muropeptide fragments larger than trimers were not observed. The *p*-
911 values for the differences between wild type and $\Delta ctpA$ strains for monomers, dimers,
912 and trimers based on the t-test are 0.0001, 0.0003, and 0.0216, respectively. (C) The
913 calculated peptidoglycan cross-linking efficiency (ρ_{CL}) for wild type and $\Delta ctpA$ mutant
914 are $50.86\% \pm 0.98\%$ and $49.46\% \pm 0.18\%$, respectively, with a *p*-value of 0.0038. All
915 errors bars represent 95% confidence interval (*n* = 3). Representative mass spectra of
916 monomer (D), dimer (E), and trimer (F) are shown with the XICs as insets. The
917 corresponding chemical structures are in Supplementary Figure S1.

918

919 **FIG 7** *In vitro* proteolysis of MepM. (A) CtpA degrades MepM and is enhanced by LbcA.
920 2 μ M of the indicated C-terminal His₆-tagged proteins were incubated for 3 h at 37°C.
921 Samples were separated on a 12.5 % SDS PAGE gel, which was stained with

922 coomassie brilliant blue. Approximate positions of molecular-mass-marker proteins
923 (kDa) are indicated on the left-hand side. (B) Time course. Reactions contained 2 μ M of
924 CtpA-His₆ and MepM-His₆ either without (-LbcA) or with (+ LbcA) 2 μ M of LbcA-His₆.
925 Reactions were terminated at the indicated time points by adding SDS-PAGE sample
926 buffer and boiling. As a negative control, the same experiment was done using PA3787
927 in place of MepM. Samples were separated on 12.5 % SDS PAGE gels, which were
928 stained with coomassie brilliant blue. Approximate positions of molecular-mass-marker
929 proteins (kDa) are indicated on the left-hand side. PA3787 ran at the midway point
930 between marker proteins of 37 and 25 kDa, which were above and below, respectively,
931 the region of the gel shown in the figure.

932

933 **FIG 8** Evidence that the LbcA•CtpA complex has additional substrates. (A) *In vivo*
934 analysis. Immunoblot analysis of equivalent amounts of whole cell lysates of wild type
935 and Δ ctpA strains, and also of Δ lbcA strains for proteins that accumulated in the Δ ctpA
936 mutant. All strains contained an arabinose-inducible expression plasmid encoding C-
937 terminal FLAG-tagged versions of the indicated proteins. Approximate positions of
938 molecular-mass-marker proteins (kDa) are indicated on the left-hand side. Test proteins
939 were detected with anti-FLAG monoclonal antibodies, and CtpA and LbcA were
940 detected with polyclonal antisera. Each box has analysis of proteins in related families,
941 as indicated at the top. Only those proteins with names in bold face accumulated in the
942 Δ ctpA mutant. (B) *In vitro* analysis. 2 μ M of the indicated C-terminal His₆-tagged
943 proteins were incubated for 3 h at 37°C. Protein only indicates incubation of the test
944 substrate alone. PA3787-His₆ was used as a negative control. Samples were separated

945 on a 15 % SDS PAGE gel, which was stained with coomassie brilliant blue.
946 Approximate positions of molecular-mass-marker proteins (kDa) are indicated on the
947 left-hand side. (C) Sensitivity of $\Delta ctpA$ and $\Delta lbcA$ mutants to low salt is not suppressed
948 by $\Delta mepM$. Strains were grown at 37°C in LB broth containing 1% (w/v) NaCl (blue) or
949 no NaCl (red). Optical density was measured hourly.

950

951 **FIG 9** Summary. In a wild type strain, CtpA forms a complex with the outer membrane
952 lipoprotein LbcA, which is required for CtpA to cleave its targets. The LbcA•CtpA
953 complex can degrade at least four enzymes predicted to cleave peptidoglycan cross-
954 links (MepM, PA1198, PA1199 and PA4404). This might provide a mechanism to
955 carefully constrain crosslink hydrolysis, limiting it to the amount needed for roles such
956 as cell elongation and/or division. In a $\Delta ctpA$ mutant, the peptidoglycan hydrolases can
957 accumulate, which causes excessive crosslink cleavage and subsequent phenotypes,
958 including a defective T3SS, enhanced surface attachment and low salt sensitivity. When
959 *mepM* is deleted from the $\Delta ctpA$ mutant, the T3SS and surface attachment phenotypes
960 revert back to wild type, suggesting that elevated MepM activity was their primary
961 cause. However, low salt sensitivity of a $\Delta ctpA$ mutant is not suppressed by $\Delta mepM$,
962 suggesting that increased activity of one or more of the other substrates is also
963 compromising cell wall integrity. OM = outer membrane, IM = inner membrane.

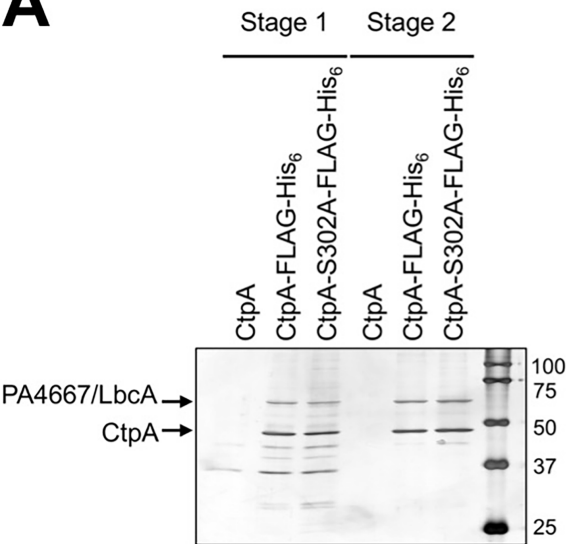
964

965 **Supplemental Table 1.** Proteins that co-purified in each of two LbcA•CtpA-S302A
966 pulldowns, but were absent in each of two LbcA•CtpA pulldowns

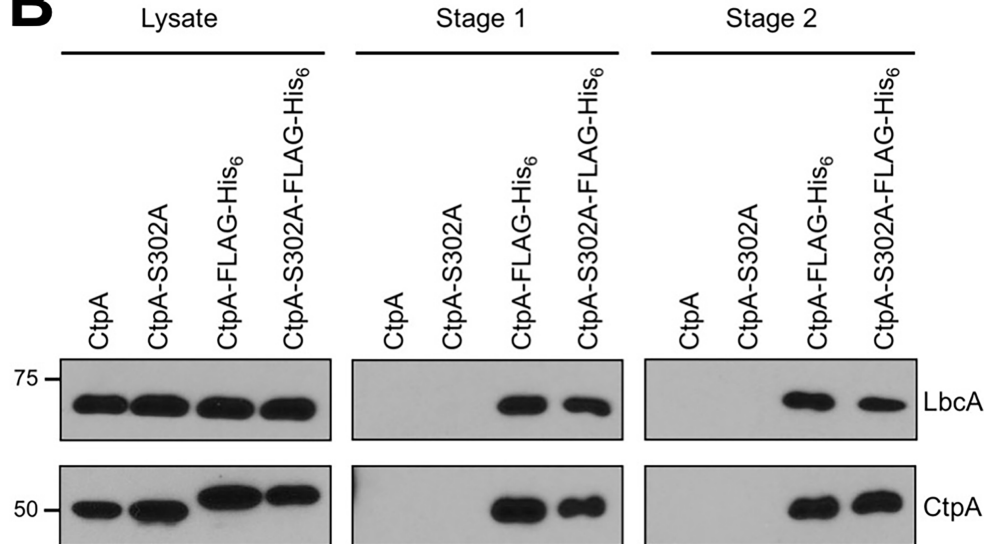
967

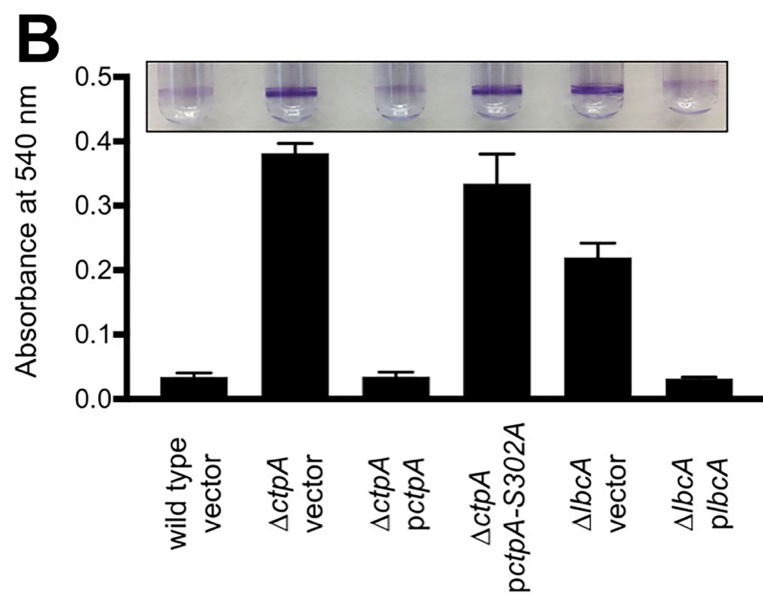
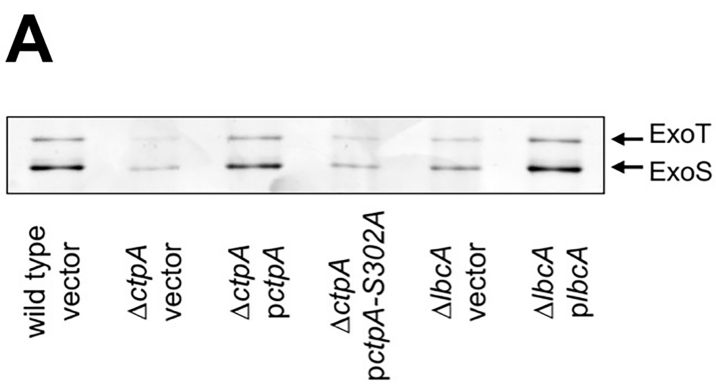
968 **Supplemental Figure S1.** Chemical structure of peptidoglycan monomer, dimer, and
969 trimer corresponding to the mass spectra shown in Figure 6

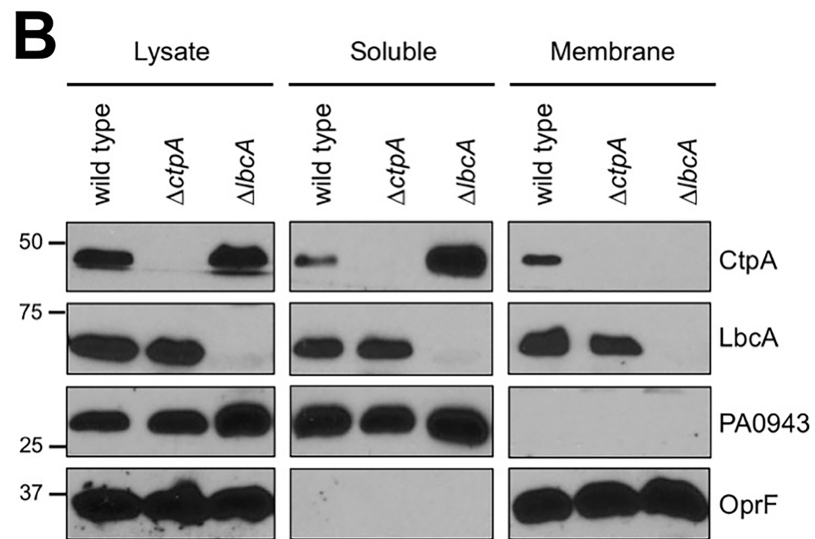
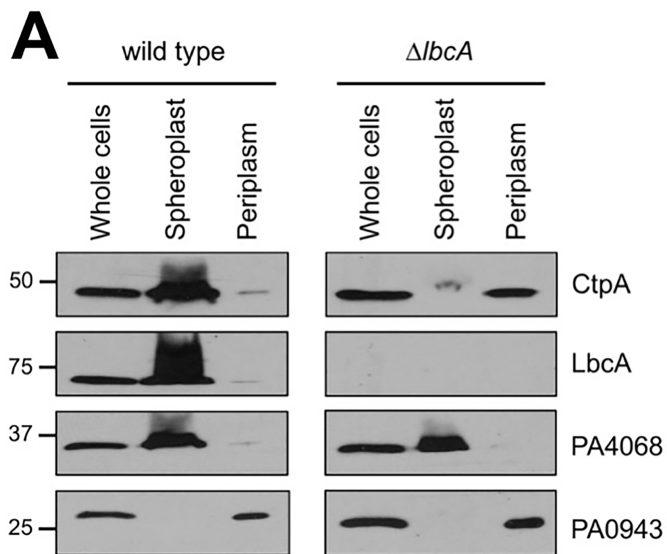
A

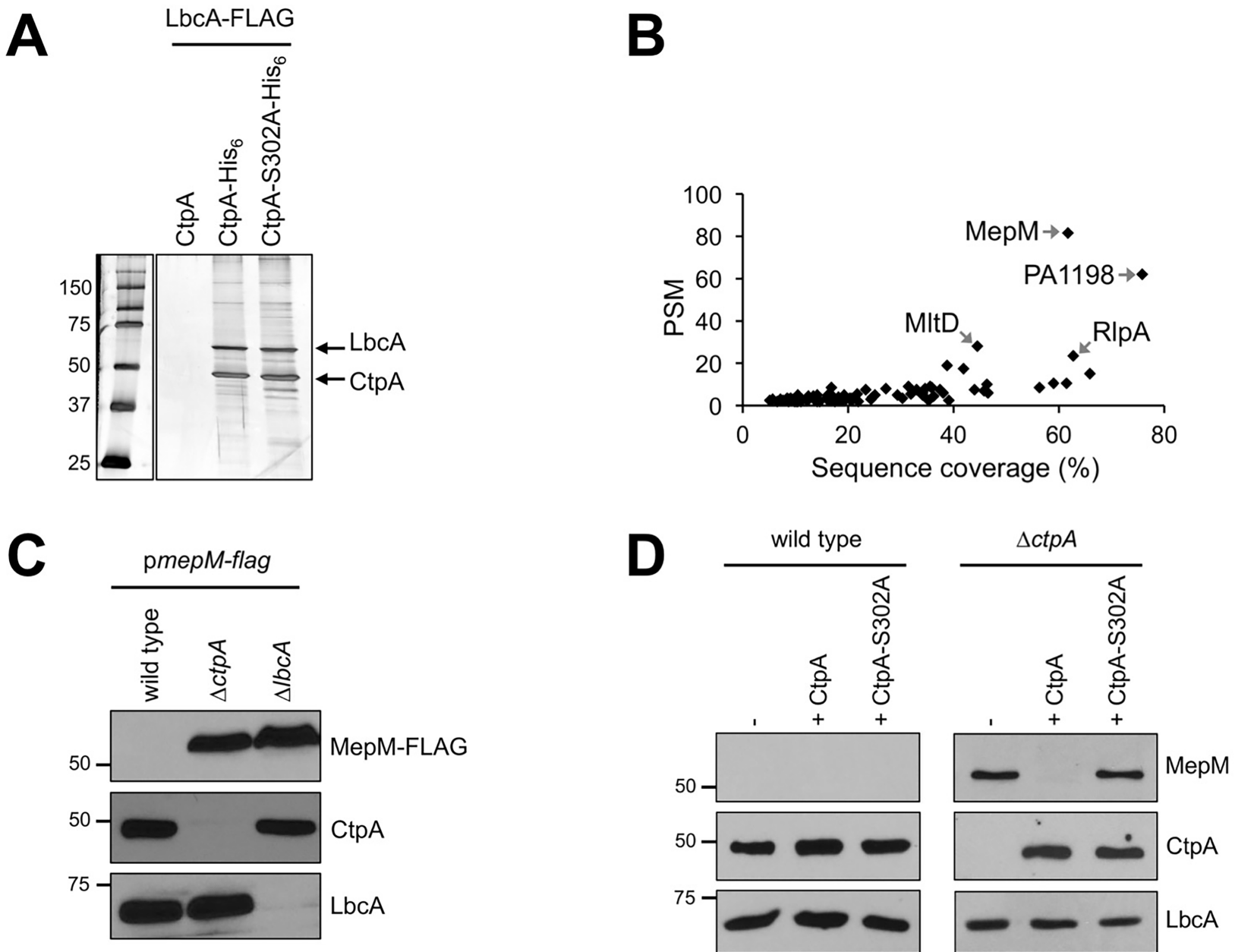


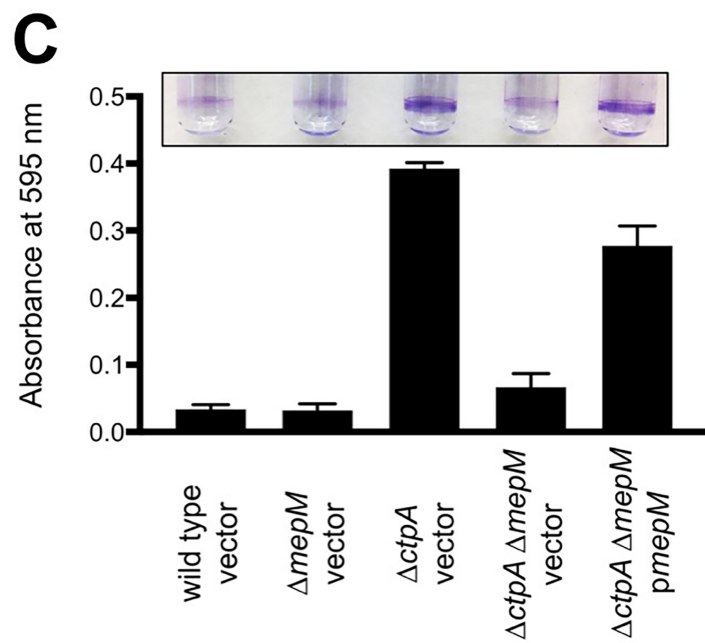
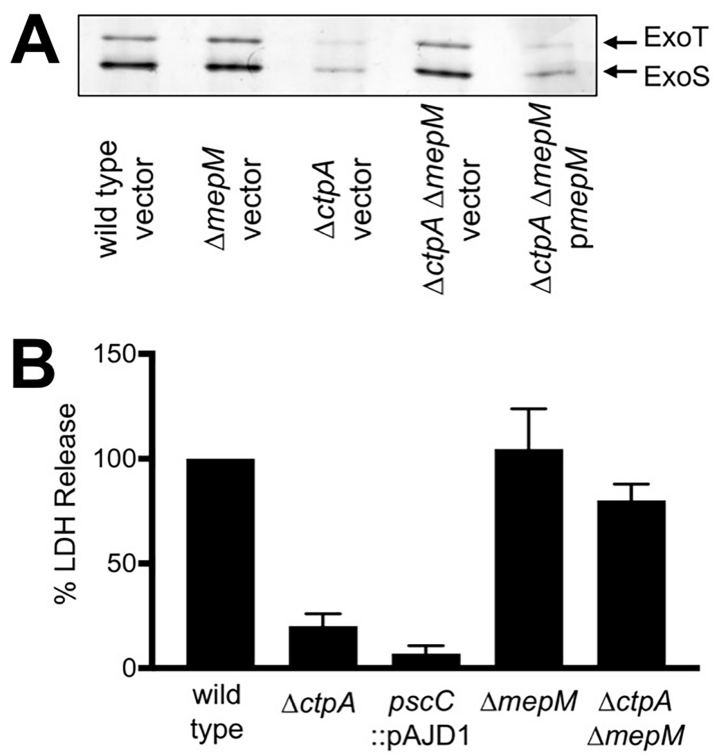
B

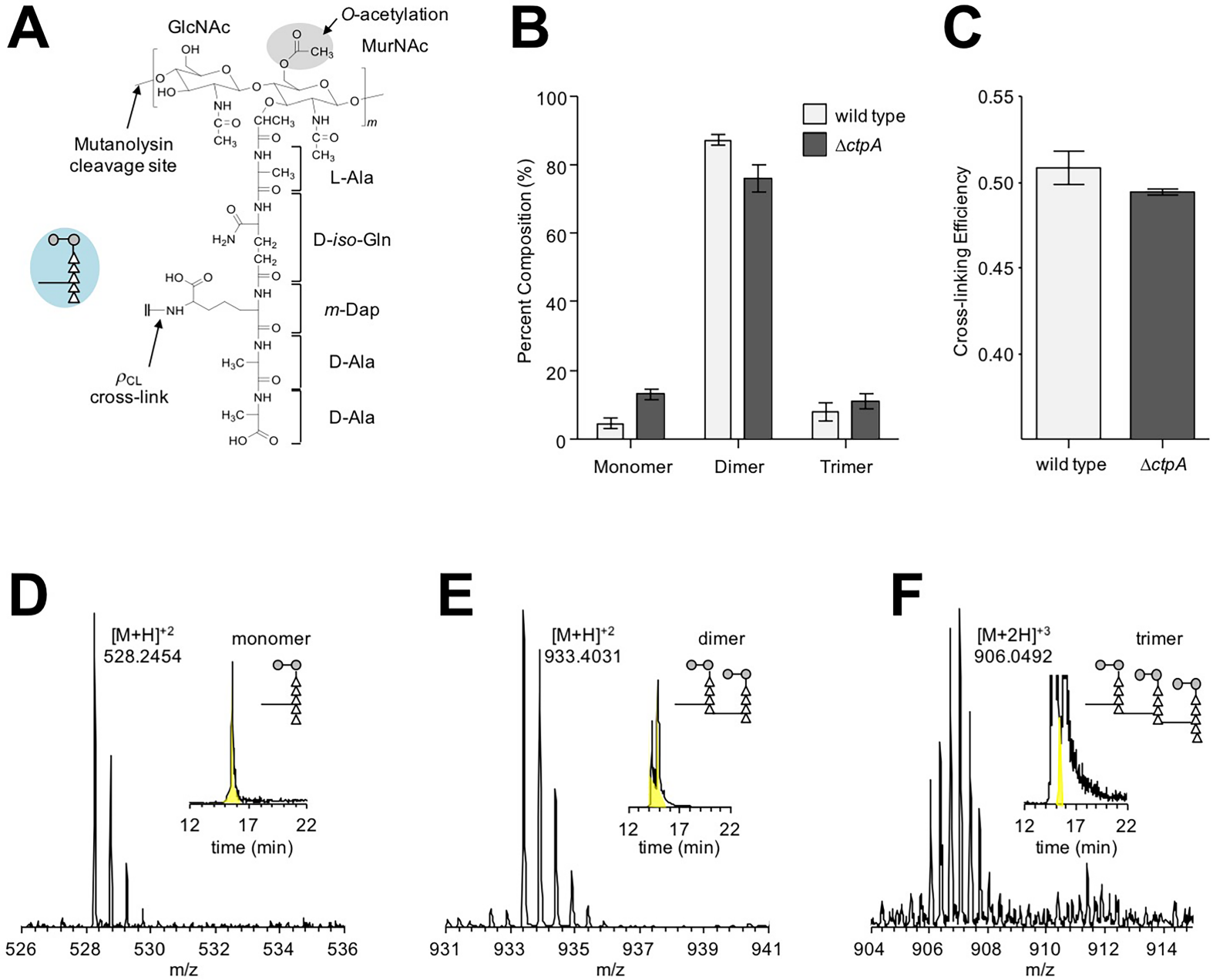


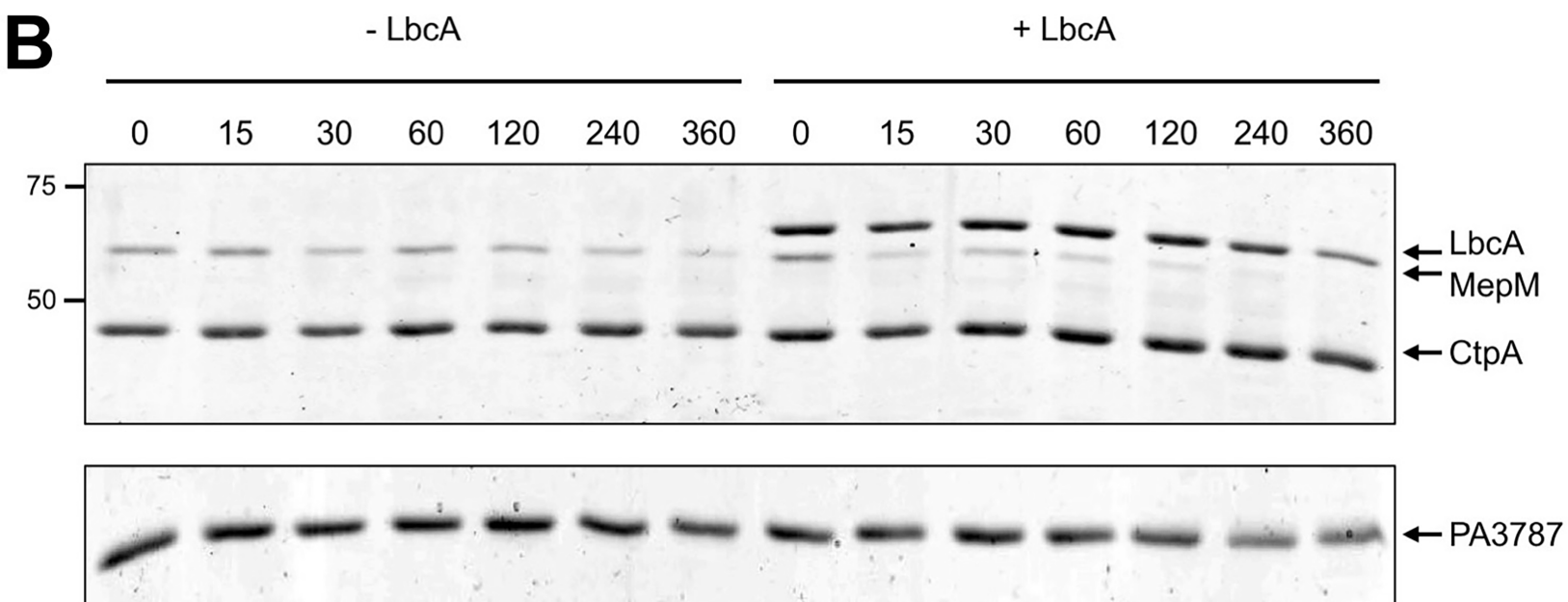
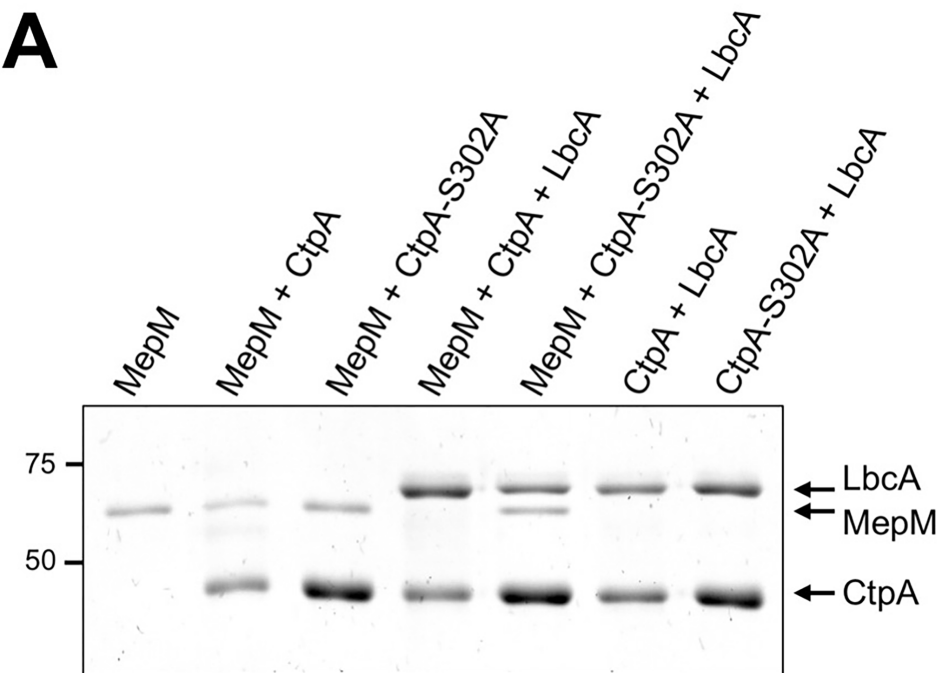




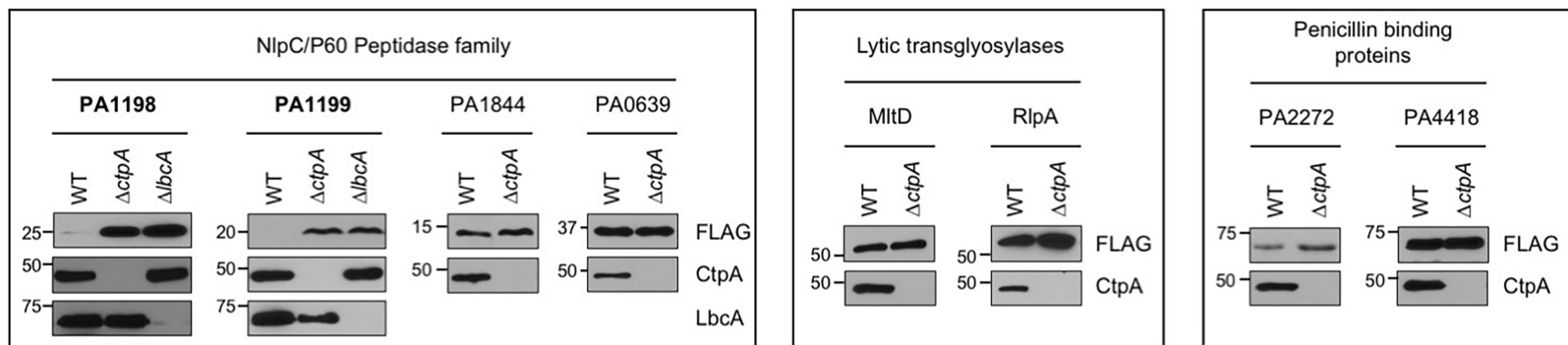
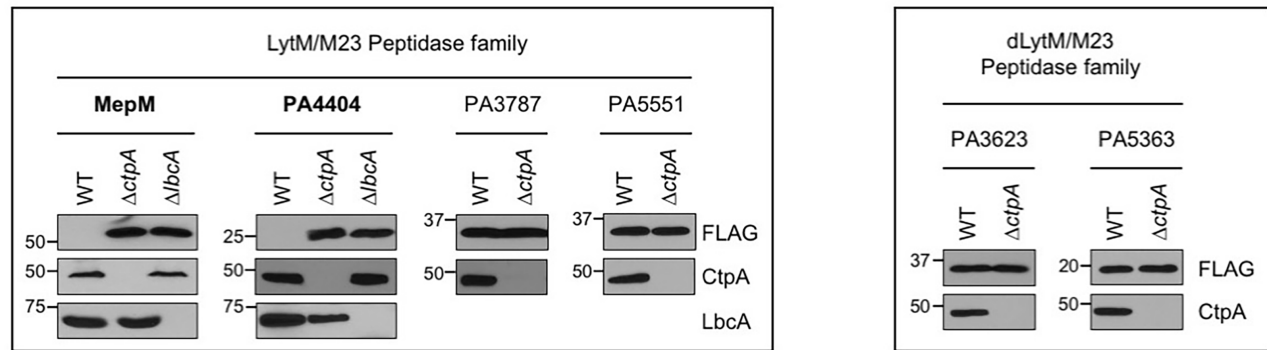




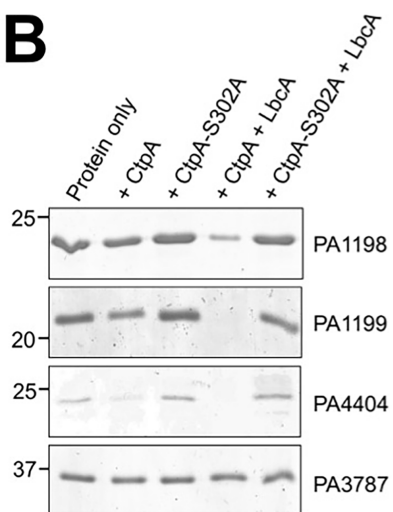




A



B



C

